Many-body localization transition with correlated disorder

Zhengyan Darius Shi,[1] Vedika Khemani,[2] Romain Vasseur,[3] and Sarang Gopalakrishnan[4]
[1]*Department of Physics, Massachusetts Institute of Technology, Cambridge, Massachusetts 02139, USA*
[2]*Department of Physics, Stanford University, Stanford, California 94305, USA*
[3]*Department of Physics, University of Massachusetts, Amherst, Massachusetts 01003, USA*
[4]*Department of Physics, The Pennsylvania State University, University Park, Pennsylvania 16802, USA*

(Received 10 May 2022; revised 29 August 2022; accepted 22 September 2022; published 5 October 2022)

We address the critical properties of the many-body localization (MBL) phase transition in one-dimensional systems subject to spatially correlated disorder. Rather than starting from a microscopic model, we analyze the transition within a strong-randomness renormalization group (RG) framework. We introduce disorder directly at the level of scaling variables appearing in the RG and consider a general family of spatial correlations, parameterized by how strong the fluctuations of the disordered couplings are when coarse-grained over a region of size ℓ. For uncorrelated randomness, the characteristic scale for these fluctuations is $\sqrt{\ell}$; more generally they scale as ℓ^{γ}. We discuss both positively correlated disorder ($1/2 < \gamma < 1$) and anticorrelated, or "hyperuniform," disorder ($\gamma < 1/2$). We argue that anticorrelations in the disorder are generally irrelevant at the MBL transition. Moreover, assuming the MBL transition is described by the recently developed renormalization-group scheme of Morningstar *et al.* [Phys. Rev. B **102**, 125134 (2020)], we argue that even positively correlated disorder leaves the critical theory unchanged, although it modifies certain properties of the many-body localized phase.

DOI: 10.1103/PhysRevB.106.144201

I. INTRODUCTION

In generic quantum many-body systems, interactions scramble local quantum information and bring subsystems towards thermal equilibrium [1–3]. This "thermalization" process fails for systems in the many-body localized (MBL) phase [4,5]. The MBL phase is best understood for systems subject to strong spatial randomness, but is also believed to occur for quasiperiodic potentials [6,7]. Systems deep in the MBL phase possess an extensive set of emergent local integrals of motion, "l bits", which leads to area-law entanglement in *all eigenstates* as well as Poisson statistics in the nearest-neighbor energy spacing distribution [8–12]. This is to be contrasted with the thermal phase that features volume-law entanglement and local energy-level repulsion conforming to random matrix theory.

While the physical picture deep inside each phase is relatively well understood, the transition between them remains mysterious. Analytically, since the transition involves singular changes in the structure of highly excited eigenstates, critical properties cannot be extracted from a conventional low energy effective field theory approach.[1] Furthermore, the lack of exactly solvable models makes it difficult to pin down key ingredients that would go into a general conceptual framework. Numerically, state-of-the-art exact-diagonalization is limited to small system sizes $L \lesssim 25$ (see, e.g., Refs. [15–19]) and produces a correlation length exponent ν that appears to violate the rigorous Harris bound $\nu \geqslant 2$ in one dimension [20–22], making any attempt to extrapolate the critical scaling difficult in the near future.

Recently, significant progress has been made by means of approximate or phenomenological real-space renormalization-group (RG) approaches [23–29]. In strongly disordered systems, one should in general consider how entire probability distributions of couplings flow as the system is coarse grained. This kind of flow fits into the general framework of *strong disorder renormalization group (SDRG)* invented by Dasgupta-Hu-Ma in Ref. [30], rigorously developed by Fisher in Refs. [31,32] and subsequently applied to numerous examples (see the review articles [33,34] for details). On the analytic side, the main appeal of SDRG is that the flow equations sometimes admit exact solutions, giving solvable models that are unavailable at the microscopic level; on the numerical side, the computational complexity of SDRGs is exponentially lower than that of exact diagonalization, allowing simulations with $O(10^7)$ initial degrees of freedom and thus providing a better chance of accessing the critical scaling.

Note that these RGs only attempt to describe the *asymptotic* MBL transition at the largest length and timescales, while the finite-size or finite-time MBL crossover observed in numerics (see Ref. [35] for recent results with correlated disorder) and experiments is believed to be described by "many-body resonances" involving rare superpositions of

[1]The MBL-thermal transition is accompanied by a transition between Poisson and Wigner-Dyson local spectral statistics. Aspects of this spectral transition can be understood from a novel effective field theory discussed, for example, in Refs. [13] and [14]. Whether or not these effective field theories can describe all the critical singularities near the transition remains an open question.

localized states that differ substantially in extensively many local regions [36–38]. We will also assume the existence of the MBL phase [8,39], see, e.g., Refs. [18,40–42] for recent discussions.

Roughly, the existing RG schemes fall into two types. The first type starts with microscopic l bits in the MBL phase, which can delocalize due to rare resonances mediated by interactions [24,26,27]. At strong disorder, resonant clusters are isolated and localization is robust. But as the disorder is reduced, resonances proliferate and tend to span the entire system, leading to thermalization.

Unfortunately, due to the complexity of the cluster formation rules, no analytic solution has been possible within the first type of RGs, thus preventing a complete understanding of the critical scaling. For this reason, we focus instead on the second type of RG scheme, which aims for analytic tractability at the expense of further coarse graining. The basic strategy is to forget about individual spins and regard the system as composed of alternating thermal (T) and insulating (I) blocks initially decoupled from each other [23]. Disorder in the microscopic couplings then translates to disorder in a few important parameters that characterize each block—the physical length, the localization length of any putative l bits it contains, the rate of entanglement growth within each block etc. [23]. When interactions between blocks are turned on, individual blocks merge into larger and larger composite blocks whose phase (T or I) and parameters are determined iteratively in terms of the parameters of their constituents. In the simplest block RG of this kind, there is a chain of blocks indexed by i, where even/odd i's correspond to T/I blocks, respectively. Each block is characterized only by its physical length $l_i^{T/I}$ and at each RG step, the shortest block gets absorbed into the surrounding blocks following a "symmetric" RG rule $l_{\text{new}}^{T/I} = l_{i-1}^{T/I} + l_i^{I/T} + l_{i+1}^{T/I}$ [25]. While completely solvable, this RG missed the important asymmetry between T and I blocks implied by the avalanche mechanism (a detailed review of avalanche will be given in Sec. III B) [43]. A followup Ref. [28] incorporated this asymmetry and obtained a family of RGs, $l_{\text{new}}^{T/I} = l_{i-1}^{T/I} + \alpha_{I/T} l_i^{I/T} + l_{i+1}^{T/I}$, controlled by the parameter $\alpha_{I/T}$. In the maximally asymmetric limit where $\alpha_I \to \infty$ and $\alpha_T \to 0$ (henceforth referred to as GVS), the important RG directions form a two-dimensional subspace in which a critical curve separates the thermal and insulating phases. The correlation length ξ is related to the distance δ from the fixed line via $\xi \sim e^{\frac{1}{\sqrt{\delta}}}$, putting GVS in the Kosterlitz-Thouless (KT) universality class. Some recent numerical studies also seem consistent with KT scaling [44–47]. (Some previous attempts to numerically extract the correlation length $\xi \sim \delta^{-\nu}$ from the RGs had found $\nu \approx 3.3$ as opposed to the KT value $\nu = \infty$, but these numerical values of ν exhibited considerable finite-size drifts.)

A modification of the GVS rules was proposed, and motivated on semimicroscopic grounds, in a paper by Morningstar and Huse [29]. In effect, this RG scheme promoted the parameter α_I in GVS to a dynamical variable that has its own RG flow. The flow of the anisotropy is motivated by the following physical picture, which we will explore in more depth in Sec. III B. Slightly on the insulating side of the MBL transition, a single small thermal block can thermalize a large insulating region (of size set by the decay length of l-bit-flip interactions) before its thermalization is eventually blocked by the discreteness of energy levels in the insulator. (At the critical point, this avalanche instead spreads throughout the system.) Thus, a typical large insulating block contains large thermal regions, through which correlations can spread without exponential suppression (i.e., that act as local short circuits for information). These short circuits renormalize the effective decay length, making it possible for a single thermal block to thermalize an even larger insulating region, and so on. Thus the anisotropy parameter α_I diverges in a specific way at the transition. The critical behavior predicted by this RG scheme was subsequently solved by Morningstar, Huse, and Imbrie [48], and we will refer to it as the MHI scheme in what follows. The critical exponent $\nu = \infty$ of MHI agrees with that of GVS, but the precise correlation length scaling $\xi \sim \delta^{-\log\log\delta^{-1}}$ differs from KT scaling. This can be traced to the nonanalytic scale dependence of the coefficients in the two-parameter MHI flow. From a general RG perspective this scale dependence seems unnatural, but it has a natural physical origin in terms of the flowing anisotropy parameter. Moreover, the MHI solution lacks certain peculiar features of the GVS solution: for example, the MHI solution predicts that thermal regions in the insulating phase have a finite fractal dimension that vanishes at the transition (consistent with rare-region counting arguments), whereas the GVS solution predicts fractal dimension zero in the MBL phase.

Since the physics of the MBL transition, within the MHI scheme, is dominated by rare regions, it is natural to ask how sensitive its unusual critical properties are to assumptions about the statistics of these rare regions. A drastic way to modify these statistics is to replace the random couplings with quasiperiodically modulated couplings. In quasiperiodic systems, rare regions (to the extent that they exist) are strongly spatially correlated, apparently invalidating many of the assumptions of MHI. Indeed, some numerical studies [6,7,49–56] and an application of the GVS RG scheme suggest that the MBL transition has a very different character from the random transition [57] (see also Ref. [58] for a different prediction using RG approaches). If in fact there are two different universality classes of the MBL transition [7], it is natural to ask whether there might be many more, corresponding to modulations that are neither conventionally random nor quasiperiodic.

In the rest of this paper we study the effects of a family of long-range (i.e., power-law) correlated disorder on the critical properties of the MBL transition.[2] In Sec. II, we review existing results and conjectures about the interplay between long-range correlated disorder and critical singularities at random fixed points, focusing on extensions of the conventional Harris bound in the presence of correlated disorder. In Sec. III B we specialize to the MHI RG rule in Ref. [48] and review the quantum avalanche mechanism that motivates it. In Sec. III D, we state the three main results of the MHI analysis for uncorrelated disorder and preview our results on

[2]see, e.g., Refs. [59–63] for previous papers on the interplay between correlated disorder and single-particle localization.

the effects of long-range correlated disorder. The key finding is that correlations do not change the characteristics of fractal thermal inclusions driving the transition and hence leave the correlation length scaling near criticality invariant. In Sec. IV, we give general arguments for the irrelevance of hyperuniform correlations in a wide class of *asymptotically additive RGs* (which includes all existing phenomonological RGs for the MBL transition). For positive correlations discussed in Sec. V, no such general argument applies. Nevertheless, using properties of the avalanche mechanism, we can still show that critical singularities of the MHI RG are stable against positive correlations, first via an intuitive physical argument in Secs. V A, V B, and then through a more rigorous analysis of the functional RG equations in Sec. V C (with some technical details relegated to the Appendices). Finally, in Sec. VI we discuss the robustness of our result to changes in the phenomenological RG rule and comment on the existence of possibly relevant perturbations (for example the quasiperiodic initial conditions considered in Refs. [57,64]).

II. LONG RANGE CORRELATIONS AND CRITICAL EXPONENTS: A BRIEF HISTORY

The interplay between correlations and criticality has a long history. The earliest papers focused on perturbations around a clean critical point, where a simple scaling argument gives a definitive stability criterion that generalizes the Harris bound [20,21,65]. Suppose the correlation length scales as $\xi \sim \delta^{-\nu}$ where δ is the deviation of the order parameter from its critical value. In the presence of disorder, δ is no longer well defined globally. Any region of linear size L can be described by the average order parameter $\bar{\delta} = \frac{1}{L^d}\sum_{i=1}^{L^d} \delta_i$ and the standard deviation $\sigma(\bar{\delta})$. In order for the correlation length scaling of the clean critical point to be stable, the fluctuation $\sigma(\bar{\delta})$ over a correlation volume ξ^d must be much smaller than the mean δ. For uncorrelated/short-range correlated disorder, $\sigma(\bar{\delta}) \sim L^{-d/2}$ by the central limit theorem. Long-range correlations generally modify this scaling to $\sigma(\bar{\delta}) \sim L^{d(w-1)}$ ($w \in [0, 1]$ is defined as the *wandering exponent*), implying a simple stability criterion $\xi^{d(w-1)} = \delta^{-d(w-1)\nu} < \delta$ or equivalently $\nu > \frac{1}{d(1-w)}$. This is the *correlated Harris bound* [66], which reduces to the usual Harris bound once we take $w = 1/2$.

However, the above bound is inadequate for inherently disordered fixed points (the MHI fixed point being an example to keep in mind). Historically, two approaches have been taken to cure this deficiency. The first approach is perturbative and only covers stability around weak uncorrelated random fixed points. The basic strategy is to perturb a clean fixed point by weak uncorrelated disorder within a replica path integral description and run the Wilsonian RG. When the disorder is weakly relevant, the theory flows to a weak uncorrelated random fixed point. After that, one adds weak correlated disorder to the uncorrelated fixed point and run the Wilsonian RG again (see Refs. [67,68] for a detailed derivation that goes through all the diagrammatics). The stability criterion thus found agrees with the *correlated Harris bound*. The second approach seeks to derive general bounds on ν for intrinsically disordered fixed points (that may or may not arise as perturbations of uncorrelated fixed points) [21,22]. The first rigorous result along this line of thinking is the Chayes-Chayes-Fisher-Spencer (CCFS) bound $\nu \geqslant \frac{2}{d}$ proven in Ref. [21] for arbitrary uncorrelated/short-range correlated disorder (including infinite randomness fixed points). For correlated disorder, the authors of Ref. [21] conjecture a *correlated CCFS bound* $\nu \geqslant \frac{1}{d(1-w)}$. If true, this bound would provide a necessary but not sufficient condition for stability, which is weaker than the *correlated Harris bound*. (For example, if the uncorrelated fixed point has exponent ν, then it is unstable against correlations with wandering exponent w when $\nu < \frac{1}{d(1-w)}$. But the bound gives no information on stability otherwise.) The stability criterion $\nu \geqslant \frac{1}{d(1-w)}$ has been checked in all SDRGs known to date (see Refs. [33,34] for comprehensive reviews). Therefore, it is conceivable that $\nu \geqslant \frac{1}{d(1-w)}$ is in fact a necessary and sufficient stability criterion for arbitrary fixed points, a conjecture that we will refer to as the *generalized Harris bound*. We emphasize that to our knowledge there is no convincing argument for the validity of the generalized Harris bound at strong-randomness fixed points.

With this historical background in mind, let us return to the MHI RG. Since the uncorrelated fixed point has $\nu = \infty$, the *generalized Harris bound* would suggest that long-range correlations with arbitrary $w \neq 1$ cannot change ν unless w flows to 1 in the IR limit. In a large class of RGs including MHI, we will explicitly calculate the flow of w and show that it does not approach 1 in the IR (see Sec. IV). Therefore, if we believe in the *generalized Harris bound*, the correlated fixed point still has $\nu = \infty$. This discussion leaves open the possibility that the fixed point might flow to a different universality class within the $\nu = \infty$ family. As the scaling theory of Ref. [69] shows, *any microscopic RG rule* with the avalanche mechanism built in must lead to KT scaling, so long as all β functions are analytic. MHI evades this argument by generating logarithmic singularities in its β functions. But since there are infinitely many types of nonanalyticities, it is natural to expect that correlations can induce a different type of singularity and give rise to a new universality class. Surprisingly, under some weak assumptions, we will show that this does not happen for any initial correlation with $w < 1$ ($w = 1$ corresponds to the unphysical case of perfect positive correlations), implying that the MHI universality class is stable. The effect of more general perturbations to the RG initial conditions (e.g., quasiperiodicity) remains an open question that we hope will be addressed in future works.

III. MODEL SETUP AND SUMMARY OF RESULTS

A. Models of correlated disorder

Before introducing the RG rules, we give a heuristic motivation for how spatially correlated disorder in a microscopic model can affect the initial conditions of the RG. For concreteness, one can have in mind the paradigmatic XYZ model

$$H = \sum_{i,\beta=x,y,z} J_\beta \sigma_i^\beta \sigma_{i+1}^\beta + \sum_i h_i \sigma_i^z, \tag{1}$$

where h_i is a set of spatially correlated random fields with variance W. Given a particular choice of correlation, we assume that there exists a critical disorder strength $W = W_c$ separating

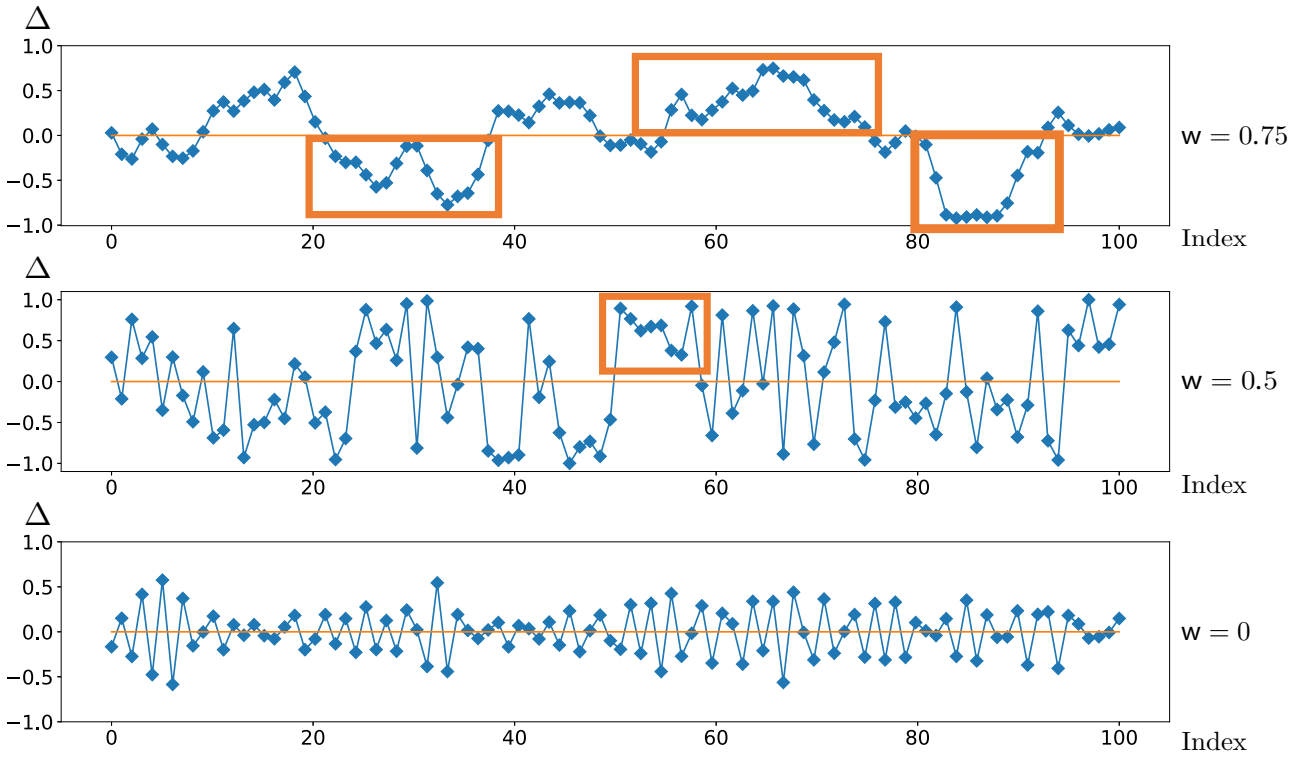

FIG. 1. Correlated disorder. From top to bottom, the three panels show three long-range correlated random sequences with wandering exponents $w = 0.75, 0.5, 0$ respectively. The vertical axis Δ measures deviation from the mean and the horizontal axis is a spatial index for sequence elements. The positively correlated sample features many long stretches of consecutive blocks on one side of the mean. The uncorrelated sample has fewer stretches, while the hyperuniform sample has strong local anticorrelation and hence no coherent fluctuation. In the RG, we impose these long-range disorder correlations directly on the block parameters. The translation between microscopic disorder and disorder in the block parameters is a complicated problem that is worth exploring in the future.

the thermal phase at weak disorder and the MBL phase at strong disorder. For every random realization of $\{h_i\}$, there are contiguous regions where every $|h_i|$ is smaller than W_c. We refer to these contiguous regions as "T blocks" (T for thermal) and the regions intervening the T blocks as "I blocks" (I for insulating). In general, the coarse-grained physical properties of each T and I block will inherit some spatial correlations from the microscopic statistics of $\{h_i\}$. Since we will be interested only in the long-distance physics near the MBL-thermal phase transition, we will directly inject spatial correlations into the coarse-grained block parameters, assuming that they arise from some more complicated unspecified correlations in $\{h_i\}$. The philosophy here is to demonstrate that critical singularities of the MHI fixed point are preserved by the most drastic long-range spatial correlations. In realistic models, the disorder correlations might be weaker and our results would continue to apply.

We now state more explicitly the forms of correlated disorder that will be used in this paper. Consider a space dependent field l_x with $\langle l_x \rangle = 0$, $\langle l_x l_y \rangle \sim W^2 C(|x-y|)$ with $C(\cdot)$ the position space correlation function normalized so that $C(0) = 1$. It is convenient to also introduce the Fourier transform of $C(x)$, which we refer to as the *correlation spectrum* $S(k) = \int e^{ikx} C(x) dx$. Throughout the analysis, we will be interested in a family of correlations with $S(k) \sim_{k\to 0} |k|^{1-2w}$ where $w \in (0, 1)$ labels the wandering exponent. When $w > 1/2$, the spatial profile $C(x) \sim |x|^{2w-2}$ is a long-range "positive correlation" and coherent fluctuations are enhanced. This is in contrast to "hyperuniform correlation" with $w < 1/2$, where the spatial profile $C(x) \sim -|x|^{2w-2}$ for all $x \neq 0$ indicates long-range anticorrelation.[3] By varying the structure of $S(k)$ near $k = 0$, we can therefore access the full range $w \in (0, 1)$ relevant for the generalized Harris bound $\nu \geqslant \frac{1}{d(1-w)}$. Some typical samples with different wandering exponents are shown in Fig. 1. In accordance with our expectations, positive/hyperuniform correlations lead to local alignment/antialignment and hence a higher/lower probability for the appearance of long sequences on one side of the average. When positive correlations are too strong, coherent fluctuations of contiguous spatial clusters are heavily enhanced, leading to a smaller effective system size. As a result, we will only be able to generate reliable samples up to $w \approx 0.85$ for $O(10^7)$ spatial sites.

[3]Numerically, one can sample from these correlated distributions by the following recipe: First draw a vector of independent Gaussians ξ_x and then consider $l_x = W\mathcal{F}^{-1}[\sqrt{S(k)} \cdot \mathcal{F}[\vec{\xi}]]$ where $\mathcal{F}$ denotes a discrete Fourier transform. If we let $q_k = \mathcal{F}(l_x)$, then it is easy to check $\langle q_k q_{-k'} \rangle = W^2 \sum_{x,y} e^{ikx} \sqrt{S(k)} e^{-ik'y} \sqrt{S(-k')} \langle \xi_x \xi_y \rangle = W^2 S(k)$. Therefore, the output of the algorithm $\vec{l}$ has the correct spatial correlation $\langle l_x l_y \rangle = W^2 C(|x-y|)$.

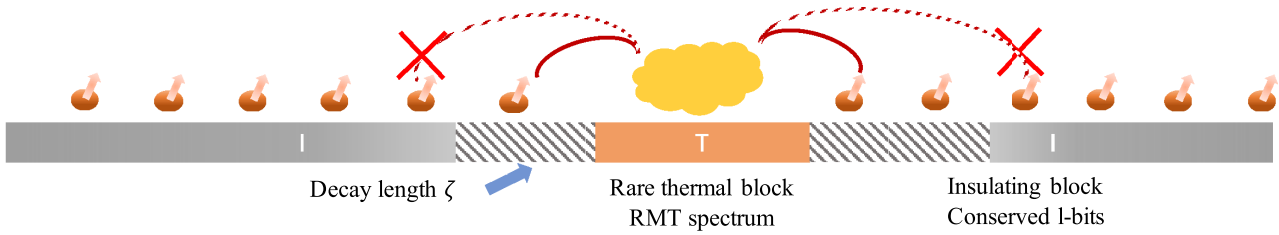

FIG. 2. Avalanche picture. The T blocks are treated as thermal baths satisfying ETH (the yellow clouds represent a swarm of scrambled microscopic degrees of freedom). The I blocks are a chain of exponentially localized l bits. The red curves represent the exponentially decaying interactions (with decay length ζ represented by the striped regions) between bath degrees of freedom and l bits in I blocks. When ζ is too large, the bath degrees of freedom thermalize the l bits closest to boundary, thus growing the T-block length until the entire I block is absorbed. When ζ is small, the T block cannot reach far beyond the boundary and the surrounding I blocks remains insulating. This is the basic physical picture for the quantum avalanche introduced in Ref. [43].

B. Motivating the MHI RG from quantum avalanche

To motivate the MHI RG rules, we give a brief review of the quantum avalanche mechanism introduced in Ref. [43]. The basic idea is to approximate each I block as a chain of conserved l bits and each T block as a fully scrambled thermal bath satisfying the eigenstate thermalization hypothesis (ETH). For exponentially local interactions, the norm of operators coupling the bath to l bits a distance x away decays as $2^{-x/\zeta}$ for some decay length ζ. Now take a T block that contains n_0 microscopic spins. Upon coupling the T block to nearby I blocks, interactions have a tendency to thermalize l bits near the boundary. But if the decay length ζ is sufficiently small, the T block may remain trapped in a sea of l bits. This heuristic reasoning suggests the existence of a critical ζ_c past, which thermalization continues indefinitely. To derive ζ_c, suppose the T block has absorbed $n/2$ l bits from each of the two nearby I blocks. Then the new bath has size $n_0 + n$. In order for the l bits further away to remain insulating, we must demand the matrix element of interactions between faraway l bits and the original thermal bath to be much smaller than the average level spacing of the bath. By the eigenstate thermalization hypothesis (ETH), the matrix element coupling the bath and the nearest surviving l bit is given by $\Gamma \sim \frac{2^{-n/(2\zeta)}}{\sqrt{2^{n_0+n}}}$[4] [1,2,43]. Comparing Γ with the level spacing of the thermal bath $\delta \sim 2^{-(n_0+n)}$, we see that the T block remains trapped iff

$$\frac{2^{-n/(2\zeta)}}{\sqrt{2^{n_0+n}}} < 2^{-(n_0+n)} \quad \rightarrow \quad -\frac{n}{\zeta} + n_0 + n < 0. \tag{2}$$

For $\zeta > 1$, the above condition can never be satisfied and the T block absorbs more and more spins like snowballs in an avalanche. Therefore the critical value is precisely $\zeta_c = 1$. We choose our length units so that n corresponds to the physical length l^I of an I block. Then by the criterion above, the shortest T block that can thermalize an I block of length l^I is given by $d = l^I(\zeta^{-1} - 1)$. Following the convention of MHI, we refer to d as the "deficit" (see Fig. 2 for a cartoon of the avalanche mechanism). Deep in the MBL phase, we expect that $\frac{d}{l^I} \rightarrow \text{const} > 0$. As the transition is approached from the MBL side, $\frac{d}{l^I} \rightarrow 0$ as T blocks eat up larger and larger I blocks, eventually taking over the entire spatial chain.

C. The recipe for MHI RG

The intuitive picture in Sec. III B immediately motivates the following RG procedure:

(1) Consider a chain labeled by an integer index $i \in \{1, \ldots, L\}$ where odd/even i corresponds to T/I blocks. For each T block, there is a single parameter l_i^T denoting the length of the T block. For each I block, there are two parameters l_i^I, d_i denoting the physical length and the deficit length. The initial sequences $\{l_i^T\}, \{d_i\}$ are two independent correlated sequences with wandering exponent w generated by the recipe in Sec. III A. The initial decay length $\zeta_0 < 1$ is chosen to be spatially uniform so that $d_i = l_i^I(\zeta_0^{-1} - 1)$ for all i. The value of ζ_0 can be used to tune across the phase transition.

(2) At each RG step, we find the cutoff $\Lambda = \min_i\{d_i, l_i^T\}$. If the shortest block is insulating, then the nearby T blocks absorb it and acquire a total physical length $l^T_{\text{new}} = l^T_{i-1} + l^I_i (= \frac{\Lambda}{x_i}) + l^T_{i+1}$ where $x_i = \zeta_i^{-1} - 1$. If the shortest block is thermal, it is too short to destabilize the nearby I blocks and therefore gets stuck in the middle (remember that d_i is the shortest T block that can thermalize the ith I block and $d_i, d_{i+1} > \Lambda$). This means we get a new I block with physical length $l^I_{\text{new}} = l^I_{i-1} + l^T_i (= \Lambda) + l^I_{i+1}$. The new deficit involves more thought. The T block that gets stuck in the middle is a seed for danger: an additional T block of length $d_{i-1} - \Lambda + d_{i+1}$ could cooperate with the T block already nested inside the new I block to destabilize all of the l bits in between. Thus, contrary to naive expectations, $d_{\text{new}} = d_{i-1} - \Lambda + d_{i+1}$ (see Fig. 3 for a pictorial representation).

(3) After each RG step, d_i/l_i^I and hence x_i will not remain uniform. So we perform an additional average over all I blocks to obtain a single value $x = \frac{1}{N_\Lambda}\sum_i x_i$ where N_Λ is the number of blocks remaining when the cutoff is Λ. Following this, we update the deficit length to $d_i = x l_i^I$.

(4) Steps 2 and 3 are repeated until Λ reaches the length scale of interest.

At first sight, the averaging procedure in step 3 has the potential to alter critical properties. But we show that this

[4]Technically what appears in the denominator should be $\sqrt{e^{S(E)}}$ where $S(E)$ is the entropy density associated with a typical infinite temperature state. But for an order of magnitude estimate, it is sufficient to approximate the denominator as $2^{D_{\text{eff}}}$ where D_{eff} is the dimension of the full Hilbert space.

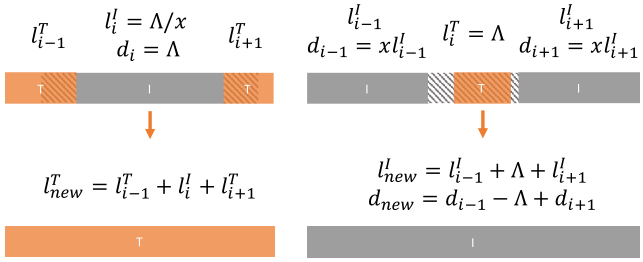

FIG. 3. RG rules. A pictorial representation of MHI RG rules. Each I block is characterized by a deficit d_i (represented by the striped region) and a physical length l^I_i (striped plus gray region), while each T block is characterized by a single physical length l^T_i (the orange region). On the LHS, the T blocks are longer than the striped region and a $ITI \to T$ follows. On the RHS, the T block in the middle is shorter than the striped region and a $ITI \to I$ ensues.

is not the case for weak inhomogeneities in x_i at some late stage in the RG: within the MBL phase, the average deficit $\langle d \rangle$ is much larger than Λ, and the average $\langle l^I \rangle$ is much larger than $\langle l^T \rangle$. Therefore, the RG rule for $ITI \to I$ move (which is the only move that can change x_i, can be approximated as $d_{\text{new}} = d_{i-1} + d_{i+1}$, $l^I_{\text{new}} = l^I_{i-1} + l^I_{i+1}$. This means that if x_{i-1}, x_{i+1} are initially close, then $\min\{x_i, x_{i+1}\} < x_{\text{new}} = (d_{i-1} + d_{i+1})/(l^I_{i-1} + l^I_{i+1}) < \max\{x_{i-1}, x_{i+1}\}$. Therefore, inhomogeneities are irrelevant under the RG flow.

Before analyzing the MHI RG in detail, we remark on some important similarities and differences between the MHI RG and the two-parameter GVS RG defined by the update rule

$$l^T_{\text{new}} = l^T_{i-1} + \alpha_I l^I_i + l^T_{i+1}, \quad l^I_{\text{new}} = l^I_{i-1} + \alpha_T l^T_i + l^I_{i+1}. \quad (3)$$

In GVS, there are two *ad hoc* parameters α_T, α_I whose ratio α_I/α_T encodes the asymmetric power of T and I blocks to absorb their neighbors. The avalanche mechanism is crudely realized as the limit where $\alpha_I/\alpha_T \to \infty$. In MHI, the ratio α_I/α_T is replaced by a much more physical parameter x^{-1}, which directly relates to the average decay length of I blocks. Furthermore, instead of imposing a diverging x^{-1} from the beginning, the MHI RG rules allow x to flow according to the avalanche mechanism. Therefore, although GVS and MHI are both motivated by the avalanche, MHI should be viewed as a significant improvement over GVS where interactions between nearby blocks are more faithfully represented.

D. Recap of MHI analysis and summary of new results

Now we turn to the analysis of the RG. The complete data at each cutoff Λ consist of a probability distribution $P_\Lambda(\{d_i\}, \{l^T_i\})$ for all remaining block parameters. When the initial condition is spatially uncorrelated, the RG procedure does not generate spatial correlations and P_Λ factorizes as

$$P_\Lambda\left(\{d_i\}, \{l^T_i\}\right) = \prod_i \rho^T_\Lambda(l^T_i)\mu^I_\Lambda(d_i) \quad (4)$$

where $\rho^T_\Lambda(l^T_i)$, $\mu^I_\Lambda(d_i)$ are the single-block marginal distributions obtained from integrating over all but one of the block parameters in P_Λ. In the continuum limit, the RG can then be formulated as PDEs for ρ^T_Λ, μ^I_Λ rather than the full P_Λ. This simplifying feature is essential to the RG solution in Ref. [48].

The main findings of their analysis can be summarized as follows:

(1) Eventually at infinite Λ and within the MBL phase, x converges to some value on the fixed line $\{x > 0\}$. The value of x determines the fractal dimension of thermal inclusions d_f and the stretching exponent of T-block lengths ϵ via $\epsilon = d_f = \frac{\log 2}{\log(x^{-1})}$. Physically, d_f is defined so that a composite T block with length l^T late in the RG is made up of microscopic T blocks with total length scaling as $(l^T)^{d_f}$. Relatedly, ϵ is defined so that $\rho^T_\Lambda(l) \sim e^{-\#l^\epsilon}$ for large l. Both d_f and ϵ measure the difficulty of generating large T blocks in the MBL phase and hence control dynamical properties whose leading contribution comes from rare T block inclusions (e.g., the conductivity).

(2) The functional RG of T-block and I-block distributions can be projected to a two-dimensional subspace spanned by the excess decay rate $x = \zeta^{-1} - \zeta_c^{-1}$ and the thermal fraction $f = \frac{\langle l^T \rangle}{\langle l^T \rangle + \langle l^I \rangle}$. For technical reasons, it is more convenient to replace f with $y = \frac{x\Lambda^2}{\langle d \rangle}\rho^T_\Lambda(\Lambda)$, which we later demonstrate to be approximately equal to f near criticality. The MBL and thermal phases meet at a critical separatrix $y(x)$ and the correlation length exponent $\nu = \infty$.

(3) The RG flow equations valid near the separatrix are given by

$$\frac{dx}{d\Lambda} = -\frac{(1+x)y}{\Lambda}, \quad y_{\Lambda/x_\Lambda} = \left(\frac{y_\Lambda}{x_\Lambda}\right)^2 \langle d \rangle \mu^I_\Lambda(\Lambda). \quad (5)$$

where $\langle d \rangle$ the expectation value of the deficit length and $\mu^I_\Lambda(\Lambda)$ is the probability density of having a deficit length precisely at cutoff. In the absence of correlations, $\langle d \rangle \mu^I_\Lambda(\Lambda) \approx 1$ at large Λ and the second equation simplifies. One can then infer the form of the separatrix $y = x^2$. For an infinitesimal perturbation δ_0 away from the separatrix, the correlation length scales as $\xi \sim \delta_0^{-\log\log\delta_0^{-1}}$, which puts uncorrelated MHI in a universality class distinct from the more familiar Kosterlitz-Thouless transition (which also satisfies $\nu = \infty$).

In the presence of correlations, technical challenges immediately arise because the full RG flow can no longer be captured by the single block marginal distributions. For hyperuniform correlations, we will give a general argument that shows their irrelevance in a class of asymptotically additive RGs (with the MHI RG as a specific example). For positive correlations, irrelevance is a special property of the MHI RG (and likely all asymptotically additive RGs based on the avalanche mechanism). Via a combination of analytic and numerical arguments, we will arrive at the following stability results parallel to the main findings of MHI:

(1) At infinite Λ, the fractal dimension of thermal inclusions in an I block is $d_f \sim \frac{\log 2}{\log x^{-1}}$ while the stretching exponent for T blocks is $\epsilon \sim \frac{\log(2-\eta)}{\log x^{-1}}$ where $0 \leqslant \eta < 1$ is a constant that cannot be determined precisely. This shows that ϵ, d_f can behave differently, although they match in the absence of correlations.

(2) The correlation length critical exponent $\nu = \infty$ is preserved.

(3) With some *additional technical assumptions*, the flow equations along and below the separatrix will continue to take the MHI form. However, positive correlations may potentially

change the value of $\langle d\rangle\mu^I_\Lambda(\Lambda)$ but do not modify the correlation length scaling, up to nonuniversal constant coefficients that are independent of Λ, δ_0.

IV. STABILITY AGAINST HYPERUNIFORM CORRELATIONS

In this section, we define a general class of *asymptotically additive RGs* (including the MHI RG as a special case) for which hyperuniform correlations in the initial block configurations do not modify the critical behavior in the vicinity of the fixed point. To arrive at this conclusion, we will argue that any initial wandering exponent $w < 1/2$ always flows back to the uncorrelated value $w = 1/2$. This fragility of hyperuniform correlations is to be contrasted with the robustness of positive correlations, whose wandering exponents generally do not flow under the same class of RGs.

We first explain the basic setup. Start with N_0 spatial sites labeled by an index i, such that microscopic blocks at site i are characterized by p positive parameters $L_{i,\alpha=1,\ldots,p}$ bounded from below by some initial RG cutoff Λ_0. In each step of the RG, these microscopic blocks combine to form larger composite blocks whose parameters are determined by a set of RG rules. The minimum of the updated block parameters sets the new cutoff Λ. We call the RG rules "asymptotically additive" if parameters of the new block can be written as a linear combination of parameters of the constituent blocks up to corrections subleading in Λ^{-1}. In other words, the updated block parameters approximately satisfy $L^{\rm new}_{i,\alpha} = \sum_{j,\beta} r_{\alpha\beta} L_{j,\beta}$ for some set of fixed constants $r_{\alpha\beta}$ independent of the spatial location. To give a concrete example, consider the symmetric RG of Ref. [25]. If we take a perspective slightly different from Sec. I and view each neighboring pair of thermal and insulating blocks as living on a single spatial site, then initially we have a correlated sequence $L_{i,1} = l^T_i$, $L_{i,2} = l^I_i$. When the shortest block is l^I_i, the spatial site i is eliminated and the spatial site $i+1$ has an updated thermal length $L^{\rm new}_{i+1,1} = L_{i,1} + L_{i,2} + L_{i+1,1} = l^T_i + l^I_i + l^T_{i+1}$; when the shortest block is l^T_i, the spatial site i is eliminated and the spatial site $i-1$ has an updated insulating length $L^{\rm new}_{i-1,2} = L_{i-1,2} + L_{i,1} + L_{i,2} = l^I_{i-1} + l^T_i + l^I_i$. All nonvanishing components of $r_{\alpha\beta}$ are equal to one in this example and we have asymptotic additivity. One can easily verify that the GVS RG of Ref. [28] and the MHI RG of Ref. [48] are also asymptotically additive with $p = 2$, $p = 3$ respectively.

We now run a general asymptotically additive RG on a spatial chain of length N_0. The initial block parameters are drawn from a translation-invariant probability distribution where for every α, $\{L_{i,\alpha}\}$ is a set of N_0 spatially correlated parameters with mean $\langle L_i\rangle = L$ (L is a constant p-component vector) and wandering exponent $0 < w < 1$. As the RG progresses to some larger cutoff Λ, the N_0 microscopic blocks are replaced by N_Λ composite blocks with parameters $\{L_{A,\alpha}\}$ where $A = 1, \ldots, N_\Lambda$. It is useful to introduce a set of integers $c(A)$ monotonically increasing with A such that the composite block A contains all microscopic blocks with initial spatial index $i \in \{c(A), c(A)+1, \ldots, c(A+1)-1\}$. In an asymptotically additive RG, the composite block parameters are approximately equal to a linear combination of parameters of microscopic blocks with $i \in \{c(A), c(A)+1, \ldots, c(A+1)-1\}$

$$L_{A,\alpha} \approx \sum_{c(A)\leqslant i<c(A+1)} \sum_\beta \tilde r_{\alpha\beta} L_{i,\beta} = \sum_{c(A)\leqslant i<c(A+1)} \tilde L_{i,\alpha}, \qquad (6)$$

where $\tilde L_{i,\alpha} = \sum_\beta \tilde r_{\alpha\beta} L_{i,\beta}$ and $\tilde r_{\alpha\beta}$ is a set of coefficients that depend on $r_{\alpha\beta}$ and the initial configuration $\{L_{i,\alpha}\}$ in some complicated way that will not be essential to the argument.

Now we think about the consequence of this additive structure for the wandering exponent w_Λ at scale Λ. Recall that w_Λ is defined such that $\sigma[\mathcal{L}_\alpha(K)] \sim K^{w_\Lambda}$ where $\sigma[\ldots]$ is the standard deviation and $\mathcal{L}_\alpha(K) = \sum_{A=1}^K L_{A,\alpha}$ is a sum over K consecutive composite blocks. Since the initial disorder distribution is translation invariant, the average composite block size $\langle c(A+1) - c(A)\rangle = S$ is independent of A and $\langle \sum_\beta \tilde r_{\alpha\beta} L_{i,\beta}\rangle = \tilde L_\alpha$ is independent of i. We thus have the following decomposition

$$\begin{aligned}
\sigma[\mathcal{L}_\alpha(K)]^2 &= \left\langle \left(\sum_{A=1}^K L_{A,\alpha} - KS\tilde L_\alpha \right)^2 \right\rangle \\
&= \left\langle \left[c(K)\tilde L_\alpha - KS\tilde L_\alpha + \sum_{i=1}^{c(K)} (\tilde L_{i,\alpha} - \tilde L_\alpha) \right]^2 \right\rangle \\
&= \langle [c(K) - KS]^2\rangle \tilde L_\alpha + \sum_{i=1}^{c(K)} \langle [\tilde L_{i,\alpha} - \tilde L_\alpha]^2\rangle \\
&\quad + 2\tilde L_\alpha \langle [c(K) - KS][\tilde L_{i,\alpha} - \tilde L_\alpha]\rangle. \qquad (7)
\end{aligned}$$

In the last line, the first term captures fluctuations in the number of microscopic blocks contained in the K composite blocks. The second term captures fluctuations in the block parameters holding the number of microscopic blocks fixed. The third term encodes correlations between these two types of fluctuations. We examine the cases $\tilde L_\alpha = 0$ and $\tilde L_\alpha \neq 0$ separately.

(1) If $\tilde L_\alpha = 0$, then only the second term of (7) survives. Since fluctuations in block parameters start out hyperuniform, there is a chance that $\{\tilde L_{i,\alpha}\}$ remains hyperuniform at all stages (we will see an example of this later). If that is the case, $\sigma[\mathcal{L}_\alpha(K)]^2 \sim c(K)^{2w} \sim K^{2w}$ and the wandering exponent w_Λ does not flow.

(2) If $\tilde L_\alpha \neq 0$ (which is the generic case), all three terms in (7) compete. Initially, there is no hyperuniformity in the number fluctuations because there is no fluctuation at all. After $n \ll N_0$ RG moves, there are $N_0 - 2n$ blocks of size 1 and n composite blocks of size 2. The number fluctuations are now directly associated with the fluctuations of spatial locations for the n smallest numbers in a hyperuniform sequence of length N_0. We checked numerically that the distribution of these locations do not inherit any hyperuniformity and the number fluctuations have wandering exponent $w = 1/2$ early in the RG. What does this mean in terms of the correlation spectrum $S(k)$? The signature of hyperuniformity is a correlation hole $S(k) \sim |k|^{1-2w}$ as $k \to 0$. Our argument above shows that a dilute set of block combinations already fill the correlation hole so that $w = 1/2$ and $S(k) \neq 0$ as $k \to 0$. To remove this constant term and restore the correlation hole requires an unphysical fine-tuning later on in the RG. Hence, even

if the second term in (7) retains hyperuniformity, the first term always wins since $K^{1/2} \gg K^w$ for $w < 1/2$. As a result, $w_\Lambda \to 1/2$ late in the RG.

In contrast, positive correlations are signaled by a singularity of $S(k)$ near $k = 0$. Numerically we find that the singularity is inherited by the number fluctuations and all three terms in (7) scale as K^{2w} with $w > 1/2$. Hence, w_Λ does not flow for positive correlations.

The above casework implies that the only way to preserve hyperuniform correlations in $\mathcal{L}_\alpha(K)$ is to have $\tilde{L}_\alpha = 0$ and $\tilde{L}_{i,\alpha}$ hyperuniform at all RG stages. In fact, a simple generalization of the above argument shows that hyperuniformity can also be preserved if a linear combination $\delta_i = \sum_\alpha t_\alpha L_{i,\alpha}$ satisfies the same properties. For general RG rules with $p > 1$ and generic $r_{\alpha\beta}$ coefficients, no such special parameter can exist. We therefore conclude that hyperuniformity is irrelevant in a generic asymptotically additive RG. Since nonlinear RG rules are even more destructive to the wandering exponents, we expect the same conclusion to hold for nonlinear RGs.

To get a concrete feel for the argument, let us consider a few examples. In the symmetric RG of Ref. [25], the basic block parameters are just the lengths l^T, l^I of T/I blocks. The RG rule is strictly additive and satisfies the assumptions in the claim:

$$l^T_{\text{new}} = l^T_i + l^I_i + l^T_{i+1}, \quad l^I_{\text{new}} = l^I_{i-1} + l^T_i + l^I_i. \tag{8}$$

At criticality, $\langle l^T \rangle = \langle l^I \rangle = O(\Lambda) \neq 0$ where Λ is the moving cutoff. Therefore, hyperuniform correlations in l^T_A, l^I_A get washed out by the number fluctuations. The only order parameter that has zero mean is $\delta_A = l^T_A - l^I_A$. But in general δ_A cannot be written as a linear combination of microscopic δ_i (this is easy to prove by contradiction). Therefore hyperuniform correlations are always irrelevant and $\nu(w < 1/2) = \nu(w = 1/2) \approx 2.5$ for every $w < 1/2$. This conclusion has been checked through finite-size scaling numerics in Appendix C.

For the random transverse field Ising model (RTFIM) with microscopic Hamiltonian $H = \sum_i J_i Z_i Z_{i+1} + \sum_i h_i X_i$, the RG parameters for each block are $\beta_i = -\log J_i$ and $\zeta_i = -\log h_i$ with cutoff $\Gamma = \log \Omega_0 - \log \Omega$ where $\Omega = \max J_i, h_i$. Late in the RG, Γ flows to infinity and $\beta_i, \zeta_i \geqslant \Gamma \geqslant 0$. The RG rules are still linear combinations of β_i, ζ_i:

$$\beta_{\text{new}} = \beta_i - \zeta_{i+1} + \beta_{i+1}, \quad \zeta_{\text{new}} = \zeta_i - \beta_{i+1} + \zeta_{i+1}. \tag{9}$$

These RG rules are identical to the symmetric RG except for the minus signs. By our general arguments, the composite block parameters $\langle \beta_A \rangle, \langle \zeta_A \rangle$ will not remain hyperuniform at large Λ. However, the special structure of the RG rules force $\delta_A = \beta_A - \zeta_A = \sum_{i \in A} \sum_i \beta_i - \zeta_i$. Since δ_A has zero mean at criticality, we must conclude that number fluctuations do not contribute and the fluctuations of δ_A *remain hyperuniform at all RG scales*! In fact, an exact solution shows that the hyperuniform RTFIM saturates the generalized Harris bound for all values of $0 < w < 1/2$ (see Ref. [70] for a complete analysis of this problem).

Finally we come to the MHI RG. Clearly, the $TIT \to T$ and the $ITI \to I$ moves are both asymptotically additive. But within the MBL phase and along the critical separatrix, the average deficit $\langle d_A \rangle, \langle l^T_A \rangle \neq 0$ and hyperuniformity in l^T_A, d_A is killed by the RG flow. Moreover, since the flow along the critical separatrix ends in the localized phase, there is an asymmetry between T and I blocks such that $\frac{\langle d_A \rangle}{\langle l^T_A \rangle} \to \infty$. This means that there cannot be a zero-mean order parameter written as a finite linear combination of d_A, l^T_A. As a result, *hyperuniform correlations are always irrelevant in the MHI RG*. For positive correlations, the wandering exponent remains different from the uncorrelated value for arbitrarily large Λ, potentially giving rise to a new universality class within the $\nu = \infty$ family. Whether or not this occurs will be explored in the next section.

V. STABILITY AGAINST POSITIVE CORRELATIONS

Positive correlations are generally relevant for asymptotically additive RG schemes. Nevertheless, for the MHI scheme (and likely other asymptotically additive RGs based on the avalanche mechanism with infinite ν at the uncorrelated random fixed point) we will find that they are irrelevant. The essential feature of avalanche-driven transitions that leads to this conclusion is that the excess interaction decay rate $x \to 0$ at the critical point. In what follows, we will specialize to the MHI scheme and argue for each of the three properties we previewed in Sec. III D: (1) that the scaling of the fractal dimension d_f is unmodified from MHI; (2) that the correlation length exponent $\nu = \infty$ for positive correlations; and (3) that (under some technical assumptions) the scaling of the correlation length is also unmodified from MHI.

A. Fractal dimension scaling survives correlations

We will use physical arguments to show that the structure of typical T/I blocks near criticality is not affected by positive correlations. This analysis will not provide a concrete understanding of the flow equations, but will be sufficient to establish the more qualitative notions of stability captured by properties (1) and (2).

The essential feature of the MHI RG that we will use is the asymmetric thermalizing powers of T and I blocks: While small T blocks can easily thermalize I blocks with large physical lengths, I blocks must start out much larger than their neighbors to remain insulating. Deep in the MBL phase, the deficit lengths d_i of the I blocks are an appreciable fraction of their physical lengths l^I_i (i.e., x is not too small). As a result, a rare T block that absorbs a neighboring I block does not grow appreciably in size and has weak thermalizing power. In order to cause an instability, we would thus need to increase the thermal fraction $f = \frac{\langle l^T \rangle}{\langle l^I \rangle + \langle l^T \rangle}$ by seeding a critical mass of T blocks. This implies the existence of a transition point f_* corresponding to every $x_* > 0$. Now suppose we decrease the value of x_*, then each T block has a higher thermalizing power and the threshold f_* should decrease. As $x_* \to 0$, f_* must also approach 0, because when $x = 0$, a single T block automatically thermalizes the whole system and no MBL phase can exist. Hence the critical point is pinned at $(x, f) = (0, 0)$ even in the presence of positive correlations. This argument is self-consistent as long as the fluctuations in $x_i = d_i/l^I_i$ are always much smaller than the mean, so that all the I blocks late in the RG can be characterized by the average x. This self-averaging property turns out to be true everywhere outside the thermal phase: Due to the asymmetric

thermalizing capacities, the MBL phase (including the critical separatrix) must satisfy $\langle L^I\rangle > \langle d\rangle \gg \langle l^T\rangle$. Recapitulating an argument in Sec. III D, the RG rule for $ITI \to I$ move (which is the only move that can change x_i), can be approximated as $d_{\text{new}} = d_{i-1} + d_{i+1}$, $l^I_{\text{new}} = l^I_{i-1} + l^I_{i+1}$. This means that if x_{i-1}, x_{i+1} are initially close, then $\min\{x_{i-1}, x_{i+1}\} < x_{\text{new}} = (d_{i-1} + d_{i+1})/(l^I_{i-1} + l^I_{i+1}) < \max\{x_{i-1}, x_{i+1}\}$, implying the irrelevance of inhomogeneities in $\{x_i\}$. The existence of a well-defined separatrix even in the presence of positive correlations has an immediate implication: if we initialize the system sufficiently close to the separatrix, we will always end up in the regime where typical I blocks have uniformly small x and large physical lengths.

As for the T blocks, living in between these gigantic I blocks is a huge challenge, and they have to fight for every opportunity to grow. Below the separatrix and within the $x, f \ll 1$ limit, the most efficient way to form large T blocks is through successive $TIT \to T$ moves where $l^T_{i-1} = l^T_{i+1} = \Lambda$ and $l^I_i = \frac{\Lambda}{x}$ at every stage. The resulting fractal structure has a fractal dimension $d_f \approx \frac{\log 2}{\log(2+x^{-1})}$, which slowly approaches zero near the critical point. Now we would like to argue that typical T blocks late in the RG have precisely this structure. If the T block lengths l^T_i were independently distributed, then the probability of growing a fractal T block of length l scales as $\exp -l^{d_f} \sim \exp -l^{\frac{\log 2}{\log x^{-1}}}$. This is to be contrasted with the probability of having a nonfractal T block of length l, which scales as $\exp -l$. As $x \to 0$, $\exp -l^{d_f} \gg \exp -l$ and hence fractal regions dominate late in the RG, precisely as shown in the uncorrelated MHI analysis [48]. In the correlated case, to establish a similar dominance, we need two crucial ingredients: (a) The probability of having a pair of neighboring T block at cutoff $C^{TT}_\Lambda(\Lambda, \Lambda)$ should approximately factorize into $\rho^T_\Lambda(\Lambda)^2$ where $\rho^T_\Lambda(l)$ is the marginal distribution of single T block lengths. (b) The presence of a T block at cutoff should not be strongly correlated with the presence of a neighboring I block at cutoff. This avoids the appearance of a long chain $TITI\ldots T$ where all I blocks are at cutoff and the whole chain merges into a single T block with $O(1)$ fractal dimension.

To argue for these "factorization"-type results, we again take advantage of the asymmetric thermalizing powers of T and I blocks. Let us consider two composite T blocks with length L^T_A, L^T_{A+1}, each containing $O(\Lambda)$ microscopic blocks. Then as $x \to 0$, the composite I block sandwiched by the T blocks contains at least $O(\frac{\Lambda}{x})$ microscopic blocks, reflecting the asymmetry. If we denote the microscopic block lengths by l_i, then by the general arguments of Sec. IV, block length correlations dominate over number fluctuations and the covariance of L^T_A, L^T_{A+1} can be approximated by

$$\begin{aligned}\left\langle L^T_A L^T_{A+1}\right\rangle_{\text{conn}} &\approx \left\langle \left(\sum_{i=1}^{\Lambda} l_i\right)\left(\sum_{j=1}^{\Lambda} l_{O\left(\frac{\Lambda}{x}\right)+j}\right)\right\rangle_{\text{conn}} \\ &\sim \sum_{i,j=1}^{\Lambda} \frac{1}{\left|O\left(\frac{\Lambda}{x}\right)+j-i\right|^c} \lesssim \Lambda^2\left(\frac{\Lambda}{x}\right)^{-c}. \quad (10)\end{aligned}$$

On the other hand, the variance of an individual composite block L^T_A is

$$\left\langle L^T_A L^T_A\right\rangle_{\text{conn}} = \left\langle \left(\sum_{i=1}^{\Lambda} l_i\right)\left(\sum_{j=1}^{\Lambda} l_{\Lambda+j}\right)\right\rangle_{\text{conn}} \sim \Lambda^{2-c}. \quad (11)$$

Comparing the two estimates above, we see

$$\left\langle L^T_A L^T_{A+1}\right\rangle_{\text{conn}} \sim x^c \left\langle L^T_A L^T_A\right\rangle_{\text{conn}}, \quad (12)$$

implying that for every $0 < c < 1$, the correlations between nearby T blocks are asymptotically suppressed in the limit $x \to 0$. This argument easily generalizes to multipoint correlations between distant composite T blocks, giving the estimate $\frac{\langle (L^T_A)^n (L^T_{A+B})^n\rangle_{\text{conn}}}{\langle (L^T_A)^{2n}\rangle_{\text{conn}}} \sim x^c/B^c$. Hence, we have a robust conclusion that the wandering exponent of T blocks $w_T \to 1/2$ as $x \to 0$, and the joint distributions of multiple consecutive T blocks should factorize into products of marginals, giving an even stronger version of ingredient (a). In contrast, the fluctuations of I block lengths retain the wandering exponent $w_I > 1/2$ of UV correlations. This is because the T block in between nearby I blocks is negligibly short and the asymptotic RG move is just successive I block additions $L^I_{\text{new}} = L^I_A + L^I_{A+1}$, which preserve the wandering exponent, as we have shown in Sec. IV.

For ingredient (b), consider now nearby T and I blocks containing Λ and Λ/x microscopic blocks respectively. Imitating the calculation before, we have

$$\left\langle \left(L^T_A\right)^n \left(L^I_{A+1}\right)^n\right\rangle - \left\langle \left(L^T_A\right)^n\right\rangle \left\langle \left(L^I_{A+1}\right)^n\right\rangle \lesssim \left[\Lambda\left(\frac{\Lambda}{x}\right)^{1-c}\right]^n. \quad (13)$$

Rewriting these correlators in terms of joint and marginal distributions and dividing by a uniform factor $x = \frac{d}{L^I}$, we have

$$\int l^n d^n C^{TI}_{\Lambda,c}(l,d) \sim \left(\frac{x}{\Lambda}\right)^{cn}\left[\int l^n \rho^T_\Lambda(l)\right]\cdot\left[\int d^n \mu^I_\Lambda(d)\right]. \quad (14)$$

The above moment estimates show that nearby T and I blocks become weakly correlated late in the RG, thereby establishing a quantitative formulation of ingredient (b). Moreover, they motivate a stronger pointwise bound $C^{TI}_{\Lambda,c}(l,d) \ll \rho^T_\Lambda(l)\mu^I_\Lambda(d)$ although no rigorous proof can be given in the absence of additional regularity assumptions. For concreteness, we provide in Fig. 4 some numerical evidence for this pointwise estimate evaluated at the cutoff $d = \Lambda$. Due to the nature of $\nu = \infty$ RGs, the critical window is extremely narrow and we cannot truly approach the $x \ll 1$ regime even for very large system sizes ($\sim 4\times 10^6$). But the trend of decaying correlations in our numerics is consistent with all the analytic arguments. We will use these facts again in the analysis of Sec. V C.

In the bottom figure, we provide an alternative visualization by fixing $l = d = \Lambda$ and tracking the evolution of $C^{TI}_{\Lambda,c}(\Lambda,\Lambda)$ as a function of Λ. One can clearly see that $|C^{TI}_{\Lambda,c}(\Lambda,\Lambda)|$ remains smaller than the product of marginals as the RG progresses, consistent with (14). The results for $C^{TT}_{\Lambda,c}$ and $C^{II}_{\Lambda,c}$ are qualitatively similar.

With ingredients (a) and (b) in hand, we return to the argument about fractal dimensions. In the presence of UV

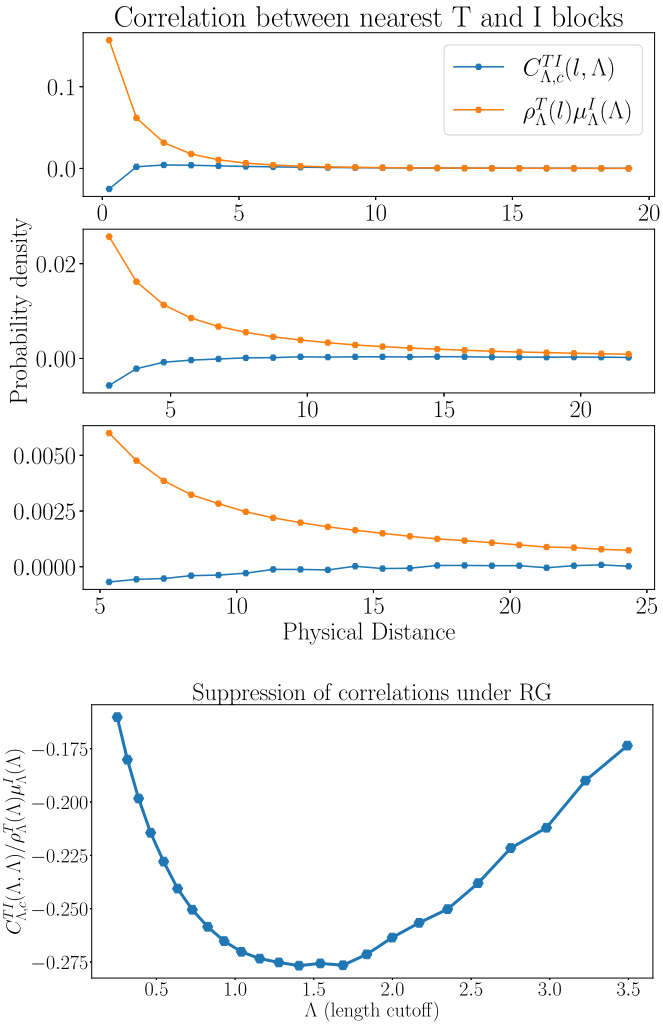

FIG. 4. Suppression of the TI correlations. In the top figure we provide some numerical evidence for (14) by plotting $C^{TI}_{\Lambda,c}(l,\Lambda)/\rho^T_\Lambda(l)\mu^I_\Lambda(\Lambda)$ against the physical separation l. We initiated the RG with 4×10^6 blocks and the top, middle, bottom panels are snapshots taken when $2\times10^6, 8\times10^5, 1.410^5$ blocks remain. Recall that correlations are suppressed when the joint distribution $C^{TI}_\Lambda(l,\Lambda)$ is close to the product of marginals $\rho^T_\Lambda(l)\mu^I_\Lambda(\Lambda)$ (or equivalently, when the connected joint distribution $|C^{TI}_{\Lambda,c}(l,\Lambda)|$ is smaller than the product of marginals).

positive correlations with decay exponent c, the probability of growing a nonfractal T block with large length l scales as $\exp -l^c$ where c is the decay exponent of the correlations. By the factorization argument above, the rare T blocks in the IR are asymptotically independent and the probability of growing a fractal inclusion of length l retains its uncorrelated scaling $\exp -l^{\frac{\log 2}{\log x^{-1}}}$. Comparing $\exp -l^{\frac{\log 2}{\log x^{-1}}}$ with $\exp -l^c$, we see that for all $0 < c < 1$, taking $x \ll 1$ always guarantees that the fractal inclusions eventually dominate over the nonfractal rare regions, thereby establishing property (1). At first sight, one may guess that d_f is equal to the stretching exponent ϵ for the T block distribution because the number of independent rare events needed to form a rare T block with length l scales as l^{d_f}. But the rarity of those events changes with scale (as pointed out by Ref. [29]) and with the flow of correlations. Hence, no precise relationship between ϵ and d_f can be inferred, although the singular scaling with x should be the same. With additional technical assumptions, we will verify in Sec. V C that this is indeed the case. In summary, the most dangerous thermalizers that prevent the rapid decay of f near the critical separatrix consist of typical T blocks in the $x, f \ll 1$ regime that are fractals with small fractal dimension. Positive correlations might affect the statistics of rare dense T blocks with larger fractal dimensions, but they play no role when we are sufficiently close to the critical point.

B. Correlation-length exponent $\nu = \infty$ survives correlations

The structure of typical T and I blocks described above also helps us understand the correlation length exponent ν. Let us define the RG time $t = \log \Lambda$, which keeps track of the exponentially large physical time elapsed during the block combination RG moves. At $t = 0$, we initialize the RG very close to the critical separatrix and with $x, f \ll 1$. In the two dimensional space (x, f), the separatrix near the fixed point (0,0) can be approximated by a curve $f(x) = x^\beta$ where β is an undetermined coefficient. To define the correlation length scaling, we slightly perturb away from the separatrix so that $f(x_0) = x_0^{\beta+\delta_0}$ for some small $\delta_0 > 0$ and ask at what RG length scale Λ does $\delta(t)$ grow to an $O(1)$ number. Within this framework, $\nu = \infty$ indicates the failure of a standard scaling ansatz $\Lambda(\delta_0) = \delta_0^{-\nu}$. For example, the Kosterlitz-Thouless transition obeys $\Lambda(\delta_0) \sim e^{b\delta_0^{-1/2}}$ and the uncorrelated MHI transition obeys $\Lambda(\delta_0) \sim \delta_0^{-\log\log\delta_0^{-1}}$. In both cases, $\Lambda(\delta_0)$ grows faster than any power law in δ_0, invaliding the hypothesis of finite ν.

Now suppose we start on the separatrix of the correlated MHI RG and slightly increase the value of x to stay in the $x \ll 1$ limit while moving below the critical separatrix. The new starting point can be regarded as a small perturbation to the correlated RG $f_0 = x_0^{\beta+\delta_0}$ where δ_0 depends smoothly on the shift of x. Note that this shift does not change the structure of fluctuations in the T/I blocks and the separatrix itself does not shift. But since positive correlations enhance coherent fluctuations, it should be more difficult for the RG flow to bring the system off criticality and the correlation length should diverge faster with δ_0. Writing the correlation length exponent $\nu(w)$ as a function of the wandering exponent w, we then expect $\nu(w > 1/2) \geqslant \nu(w = 1/2)$. In the $x, f \ll 1$ regime, the uncorrelated MHI RG already has $\nu = \infty$. Hence we expect $\nu = \infty$ for positive correlations as well.

To illustrate this general picture, we can analyze the fractal inclusions that drive the critical fluctuations more carefully. Each time a rare I block at cutoff gets absorbed by the nearest T blocks, the new T block that forms has length $O(\frac{\Lambda}{x})$. Slightly off criticality and in the MBL side of the separatrix, these are the dominant processes that prevent T blocks from completely vanishing. Hence we can basically run the RG in discrete steps, where the cutoff gets moved from $\Lambda \to \frac{\Lambda}{x}$ in each step. If we denote the number of such discrete RG steps by n, then $\frac{\Delta t}{\Delta n} = \log x^{-1}$. Along the separatrix, due to critical slowing down, $x(t)$ is an inverse power law in t and $\log x^{-1} \sim \log t$. Therefore, upon integration, the total RG time T is related to the total number of discrete RG steps by

$T \sim N \log N$ up to subleading corrections. Now we start with a small deviation δ_0 from the separatrix and suppose that $\delta(t)$ becomes $O(1)$ when $t = T(\delta_0)$. Using the definition of ν, we then conclude that

$$\Lambda(\delta_0) \sim e^{T(\delta_0)} \sim e^{N(\delta_0)\log N(\delta_0)} \sim \delta_0^{-\nu} = e^{\nu \log \delta_0^{-1}}. \quad (15)$$

If $\nu < \infty$, the above equation implies $\delta(n) \sim e^{n \log n}$, which is faster than the exponential growth $\delta(n) \sim e^n$ seen in the uncorrelated MHI RG. In order to have such a super-exponential growth, the fractal thermal inclusions controlling the transition would have to be easier to suppress in the system with positive correlation than in an uncorrelated system. This is opposite from the physical intuition that positive correlations enhance coherent fluctuations (i.e., in this case the coherent fluctuations are just the random production of larger and larger fractal T blocks). As a result, $\nu = \infty$ continues to hold for positive correlations and property (2) is established. One caveat of the above reasoning is that positive correlations modify the location of the separatrix and a direct comparison of the scaling ansatzes for uncorrelated and correlated RGs is not strictly justified because δ_0's are defined with different reference points. We will address these and other subtle issues in the next section.

C. Precise argument for correlation-length scaling based on the hierarchy of flow equations

The preceding intuitive discussion explains why positive correlations are irrelevant on the level of typical fractal block structures and correlation length exponent ν. However, even if these results are true, there is no reason to expect that the universality class of the transition also remains unmodified. As we have seen, the correlation length scaling is determined by the rate at which a small perturbation δ_0 away from the critical separatrix increases with the number of fractal steps n. Since positive correlations are expected to suppress the growth of δ_0 with n, it is in principle possible that they modify the uncorrelated MHI scaling $\delta(n) \sim e^n$ to the KT scaling $\delta(n) \sim \log n$ observed in earlier RG studies [28,69]. In fact, as we will see, when connected correlators $C^{TI}_{\Lambda,c}(l,d)$ and their higher-order analogues are sufficiently large, the asymptotic flow equations projected to the two-parameter space will indeed have a different structure. Nevertheless, under suitable assumptions that are supported by analytics and numerics, the change in flow equations leaves the exponential scaling of $\delta(n)$ invariant, thereby confirming property (3).

To prepare for this technical analysis, we begin by introducing some notations. As explained already in Sec. III D, the RG equations form an infinite hierarchy where the flow of joint probability distributions for n nearest-neighbor blocks is controlled by a functional involving $n+2$ nearest-neighbor blocks. While this infinite hierarchy of equations is difficult to solve, a lot of progress can be made by concentrating on the few-body correlations. Following the convention of Ref. [48], we first consider the marginal distributions $\rho^T_\Lambda(l)$, $\mu^I_\Lambda(d)$ of single-block lengths obtained from integrating out all but one of the blocks in the full joint probability distribution $P(\vec{d})$, $P(\vec{L}^T)$ (by translation invariance the choice of blocks to integrate over does not matter). By counting the different kinds of decimations that can occur at every RG step, we have the following flow equations:

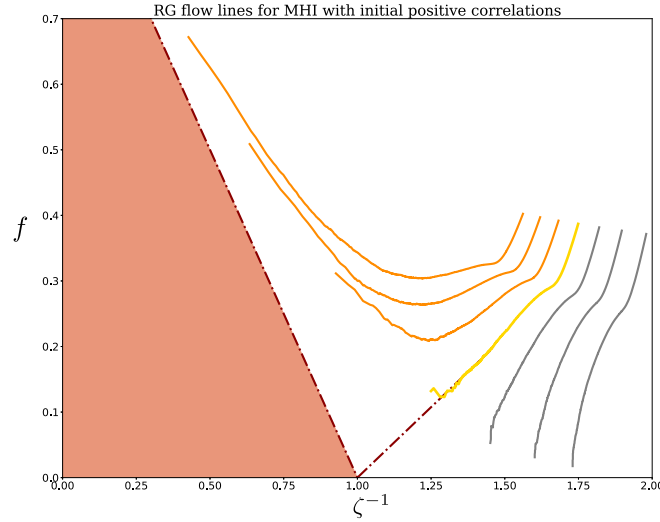

FIG. 5. Numerical RG flow. Flow lines of the MHI RG with $w = 0.75$ and initial system size $N = 4 \cdot 10^6$. The horizontal axis ζ^{-1} is the average inverse decay length and the vertical axis f is the thermal fraction $\langle l^T\rangle/(\langle l^T\rangle + \langle l^I\rangle)$. The different flows correspond to initial values of ζ between $0.245 \sim 0.305$ in steps of 0.01. The yellow critical flow separates the orange/grey flows, which land in the T/I phase respectively. The ultra-thermal shaded region is inaccessible given the finite density of l bits to start with.

$$\partial_\Lambda \rho^T_\Lambda(l) = \rho^T_\Lambda(l)\big[\mu^I_\Lambda(\Lambda) + \rho^T_\Lambda(\Lambda)\big] - 2C^{TI}_\Lambda(l,\Lambda) + \int_\Lambda^{l-\frac{\Delta}{x}-\Lambda} C^{TIT}_\Lambda\Big(l_1, \Lambda, l - \frac{\Lambda}{x} - l_1\Big) dl_1, \quad (16)$$

$$\partial_\Lambda \mu^I_\Lambda(d) = \mu^I_\Lambda(d)\big[\mu^I_\Lambda(\Lambda) + \rho^T_\Lambda(\Lambda)\big] - 2C^{TI}_\Lambda(\Lambda,d) + \int_\Lambda^d C^{ITI}_\Lambda(s,\Lambda,d+\Lambda-s)ds. \quad (17)$$

These equations differ from MHI due to the appearance of two-block and three-block joint distributions on the right-hand side (RHS). In the absence of correlations, all joint distributions factorize into products of marginals and we recover a closed set of PDEs for $\rho^T_\Lambda(l)$, $\mu^I_\Lambda(d)$ as in MHI. Once we turn on correlations, the equations no longer close, and we need to do more work. Fortunately, from Sec. V A, we know that the phase transition is controlled by a competition between the tendency of T blocks to proliferate and the presence of an excess decay rate $x > 0$ that protects l bits in the I block. This competition can be understood by projecting the infinite-dimensional flow to a two-dimensional subspace (x, f) as long as there is no additional relevant RG direction. We verify this numerically by plotting the numerical RG flow lines for different initial conditions and showing that they have no crossing down to the largest length scales. An example of this numerical check is shown in Fig. 5 for $w = 0.75$ and initial system size $L = 4\times10^6$.

Since the thermal fraction f is awkward to work with for technical reasons, we introduce a rescaled variable y defined

TABLE I. Notation for important variables.

T-block length	I-block length, deficit length	Excess interaction decay rate	Proxy for thermal fraction	Marginal distribution	Joint distribution	Fractal dimension
l^T/l	l^I, d	$x = \frac{\langle d\rangle}{\langle l^I\rangle} = \zeta^{-1} - 1$	$y = \Lambda^2 r_\Lambda(\Lambda)$	$\rho^T_\Lambda(l), \mu^I_\Lambda(d)$	$C^{TI\ldots T}_\Lambda(l_1, \ldots)$	d_f

as follows:

$$x = \frac{\langle d\rangle}{\langle l^I\rangle}, \quad y = \Lambda^2 r_\Lambda(\Lambda), \quad r_\Lambda(l) = \frac{x}{\langle d\rangle}\rho^T_\Lambda(l). \tag{18}$$

In the insulating phase,

$$f = \frac{\langle l^T\rangle}{\langle l^I\rangle + \langle l^T\rangle} \approx \frac{\langle l^T\rangle}{\langle l^I\rangle} = \frac{x}{\langle d\rangle}\int_\Lambda^\infty l\rho^T_\Lambda(l)dl. \tag{19}$$

Along the separatrix, we will later show that $\Lambda^2\rho^T_\Lambda(\Lambda) \approx \langle l^T\rangle$, implying the asymptotic equivalence between f and y at large Λ. Below the separatrix, $\langle d\rangle$ grows as a stretched exponential in Λ and y, f both tend to zero. Therefore, one can loosely think about y as a "proxy for the thermal fraction". These and other notations are summarized in Table I for convenient reference.

Some qualitative features of this projected RG flow are now transparent. In the insulating phase, $f \to 0$ and $y \to 0$ as I blocks dominate over T blocks. A finite excess decay rate x persists to infinite Λ and we land somewhere on the MBL fixed line $x > 0, y = 0$; in the thermal phase, $f \to 1$ and $y \to \infty$ as $\langle l^T\rangle \gg \langle L^I\rangle$. Therefore, we expect a "critical separatrix" in (x, y) marking a phase transition. To study this separatrix and the critical scaling close to it, we need to derive flow equations for x and y. The flow equation for x requires only a single lemma:

Lemma V.1. The form of the flow equations for marginal expectation values $\langle l^T\rangle, \langle L^I\rangle, \langle d\rangle$ are unmodified by correlations.

The proof of this lemma involves a tedious calculation, which we include in Appendix A. Here, we will merely quote the results,

$$\frac{d\langle L^I\rangle}{d\Lambda} = \mu^I_\Lambda(\Lambda)\left[\langle L^I\rangle - \frac{\Lambda}{x}\right] + \rho^T_\Lambda(\Lambda)[\langle L^I\rangle + \Lambda], \tag{20}$$

$$\frac{d\langle l^T\rangle}{d\Lambda} = \rho^T_\Lambda(\Lambda)[\langle l^T\rangle - \Lambda] + \mu^I_\Lambda(\Lambda)\left[\langle l^T\rangle + \frac{\Lambda}{x}\right], \tag{21}$$

$$\frac{d\langle d\rangle}{d\Lambda} = \left[\mu^I_\Lambda(\Lambda) + \rho^T_\Lambda(\Lambda)\right](\langle d\rangle - \Lambda). \tag{22}$$

It is important to remark that this is a "not" a closed set of equations for the averages $\langle L^I\rangle, \langle l^T\rangle, \langle d\rangle$ because the RHS involves the marginal distributions. Therefore, although these equations are formally equivalent to those in MHI, they are sensitive to correlations through the flow of single-block marginals on the RHS.

With this difference in mind, we proceed to work out the flow equations for x and y. The flow equation for x follows easily from the flow equations for expectation values derived above:

$$\begin{aligned}\frac{dx}{d\Lambda} &= \frac{1}{\langle l^I\rangle}\frac{d\langle d\rangle}{d\Lambda} - \frac{\langle d\rangle}{\langle l^I\rangle^2}\frac{d\langle l^I\rangle}{d\Lambda}\\ &= \frac{1}{\langle l^I\rangle}\left[\mu^I_\Lambda(\Lambda) + \rho^T_\Lambda(\Lambda)\right](\langle d\rangle - \Lambda)\\ &\quad - \frac{\langle d\rangle}{\langle l^I\rangle^2}\left(\left[\langle l^I\rangle - \frac{\Lambda}{x}\right]\mu^I_\Lambda(\Lambda) + (\langle l^I\rangle + \Lambda)\rho^T_\Lambda(\Lambda)\right)\\ &= \frac{-\Lambda(1+x)x\rho^T_\Lambda(\Lambda)}{\langle d\rangle} = -\frac{(1+x)y}{\Lambda}.\end{aligned} \tag{23}$$

The flow of $y = \Lambda^2 r_\Lambda(\Lambda)$ will follow from the flow of $r_\Lambda(l)$, which is simple to derive using the flow of $\rho^T_\Lambda(l)$, $\langle d\rangle$ in (16) and (22) (see Appendix B for details),

$$\begin{aligned}\partial_\Lambda r_\Lambda(l) &= \left(-\frac{y}{\Lambda} + \frac{\Lambda\mu^I_\Lambda(\Lambda)}{\langle d\rangle} - \frac{2C^{TI}_\Lambda(l,\Lambda)}{\rho^T_\Lambda(l)}\right)r_\Lambda(l)\\ &\quad + \frac{x}{\langle d\rangle}\int_\Lambda^{l-\Lambda(1+x^{-1})} C^{TIT}_\Lambda(l_1, \Lambda, l - \Lambda/x - l_1)dl_1.\end{aligned} \tag{24}$$

In the absence of correlations, MHI was able to integrate this flow and obtain a recursion relation that estimates $r_\Lambda(\Lambda/x)$ based on knowledge of $r_\Lambda(\Lambda)$. This recursion, combined with the flow of x, then gives a complete understanding of the critical separatrix and small perturbations around it. Crucially, this recursion relies again on the fact that C^{TIT}_Λ factorizes into a product of marginals so that the left-hand side (LHS) and RHS can be related to the marginals evaluated at different RG scales. In the presence of correlations, factorization is no longer possible and a recursion of r_Λ requires a different argument, which we now summarize.

First we make the general decomposition $C_\Lambda = C_{\Lambda,\text{disc}} + C_{\Lambda,c}$ where $C_{\Lambda,\text{disc}}$ is a product of marginal distributions and $C_{\Lambda,c}$ is the connected part, which vanishes in the absence of correlations. Under "three fundamental assumptions", we will show that the first term on the RHS of (24) is negligible when we integrate from $\Lambda = x^2 l$ and $\Lambda = xl$, even when the connected correlators $C_{\Lambda,c}$ are larger than C_{disc}. Within the same integration range and using the same assumptions on $C_{\Lambda,c}$, we then argue that for positive correlations, although the integrand cannot be factorized, the full integral nonetheless reduces to the factorized answer (an intuitive justification of this fact will be provided along the way). These arguments would produce a recursion in r_Λ that differs from the MHI answer. In the final step we show that the modified recursion can lead to a shifted stretching exponent ϵ inside the MBL phase but cannot change the fractal dimension d_f or the correlation length scaling, providing a precise extension of the results in Sec. V A. Throughout the argument, we will state various technical lemmas and provide some intuition. But the proofs for these lemmas are relegated to Appendix B.

The first assumption we make is a generic property of systems driven to criticality:

Assumption 1: Critical slowing down holds along the separatrix so that $x \sim t^{-\alpha}$ for some positive exponent α where $t = \log \Lambda$ is the RG time. In the uncorrelated MHI RG, $\alpha = 1$. Here we only assume that α is finite.

This is physically very reasonable because fluctuations become more and more macroscopic near the critical point at $(x, y) = (0, 0)$ and relaxation of these macroscopic regions to equilibrium takes longer and longer. In the language of renormalization group, the fastest term in the β function (which gives rise to exponentially fast growth/decay) vanishes along the critical separatrix and the subleading terms take over to give a power law behavior. Surprisingly, critical slowing down alone already provides a powerful constraint:

Lemma V.2. Under assumption 1, $\langle d \rangle \sim \Lambda \log \Lambda \gg \Lambda$, $\mu^I_\Lambda(\Lambda) < x \rho^T_\Lambda(\Lambda)$, $\rho^T_\Lambda(\Lambda) \approx \frac{1}{\Lambda} + O(\frac{1}{\Lambda \mathrm{Poly}(\log \Lambda)})$ in the large Λ limit along the critical separatrix. Below the critical separatrix (in the MBL phase), $\langle d \rangle \gg \Lambda$ and $\mu^I_\Lambda(\Lambda) < x \rho^T_\Lambda(\Lambda)$ still hold.

A direct implication of this lemma is the slow decay of x with Λ near the critical separatrix. To see this, we recall the general flow equation (23) for x,

$$\frac{dx}{d\Lambda} = -\Lambda(1+x)x\frac{\rho^T_\Lambda(\Lambda)}{\langle d \rangle} \approx -\frac{\Lambda \rho^T_\Lambda(\Lambda)}{\langle d \rangle} x. \tag{25}$$

Along the separatrix, Lemma V.2 implies $\langle d \rangle \sim \Lambda \log \Lambda$ and $\rho^T_\Lambda(\Lambda)$, consistent with the logarithmically slow growth rate of x. Below the separatrix, $\rho^T_\Lambda(\Lambda)$ becomes larger than $\rho^T_{\Lambda,\mathrm{crit}}(\Lambda)$ as T blocks are more likely to be decimated. But $\langle d \rangle^{-1}$ decays exponentially fast in $\int^\Lambda \rho^T_{\Lambda'}(\Lambda') d\Lambda'$. Therefore, the decay of $\langle d \rangle^{-1}$ overwhelms the growth of $\rho^T_\Lambda(\Lambda)$ and $\frac{dx}{d\Lambda}$ also becomes much smaller. As a result, the assumption of slow change in x can be justified everywhere outside the thermal phase, a property that we will use repeatedly later.

Despite its power, this lemma only gives information about the marginal distributions precisely evaluated at the cutoff and strictly along the separatrix. A more quantitative understanding of the RG flow requires two additional assumptions:

Assumption 2: Along and below the critical separatrix, as the I blocks become much longer than the T blocks, the distribution of deficit lengths $\mu^I_\Lambda(d)$ for I blocks tends to become wider and flatter. Concretely, we will assume that $\mu^I_\Lambda(\Lambda)$ decreases with Λ and the derivative $\partial_d \mu^I_\Lambda(d)$ evaluated at the cutoff $d = \Lambda$ goes to zero sufficiently rapidly as $\Lambda \to \infty$:

$$-\partial_d \log \mu^I_\Lambda(d), -\partial_d \log C^{TIT}_\Lambda(l_1, d, l_2)\big|_{d=\Lambda} \ll \rho^T_{\Lambda,\mathrm{crit}}(\Lambda). \tag{26}$$

What appears on the RHS is the probability of having T blocks at cutoff along the critical separatrix. In the uncorrelated RG, $\mu^I_\Lambda(d)$ is an exponential distribution and one can easily show that

$$-\partial_d \log \mu^I_\Lambda(d)\big|_{d=\Lambda} \sim \mu^I_\Lambda(\Lambda). \tag{27}$$

When we turn on correlations, we allow the distribution to change in form, but we relax the right hand side to $\rho^T_{\Lambda,\mathrm{crit}}(\Lambda)$. This should be regarded as a weak assumption because T-block decimation always dominates along the separatrix, implying $\mu^I_{\Lambda,\mathrm{crit}}(\Lambda) \ll \rho^T_{\Lambda,\mathrm{crit}}(\Lambda)$. Below the separatrix, I blocks at cutoff become even rarer and the inequality becomes more strongly satisfied.

Assumption 3: The connected distributions of nearest-neighbor T and I blocks are upper bounded by a function that is much larger than the product of marginal distributions for $l \in [\Lambda, \Lambda/x]$,

$$\left|\frac{C^{TI}_{\Lambda,c}(l,\Lambda)}{\rho^T_\Lambda(l)\mu^I_\Lambda(\Lambda)}\right|, \left|\frac{C^{TITI}_{\Lambda,c}(l_1,\Lambda,l_2,\Lambda)}{C^{TIT}_\Lambda(l_1,\Lambda,l_2)\mu^I_\Lambda(\Lambda)}\right| \ll \frac{\rho^T_{\Lambda,\mathrm{crit}}(\Lambda)}{\mu^I_\Lambda(\Lambda)}. \tag{28}$$

As we have argued in Sec. V A, correlations between nearby T and I blocks should be washed out in the sense that joint moments approximately factorize $\langle l_i^n d_j^m \rangle \approx \langle l_i^n \rangle \langle d_j^m \rangle$. However, convergence of moments do not really imply pointwise convergence of probability distributions. This is the key difficulty that necessitates the introduction of additional assumptions that impose pointwise bounds on the connected correlators. To maximize the robustness of our arguments, we allow the connected correlators to be much larger than the product of marginals pointwise but much smaller than the product of marginals multiplied by $\frac{\rho^T_{\Lambda,\mathrm{crit}}(\Lambda)}{\mu^I_\Lambda(\Lambda)}$. Along the critical separatrix, this additional multiplicative factor diverges as a power law in $t \equiv \log \Lambda$. Below the separatrix, it diverges even faster since I blocks at cutoff become stretched-exponentially rare.

With these weakened assumptions, the asymptotic projected flow equations for x, y could be significantly modified. Nevertheless, the correlation length scaling does not change. To show this, we continue the analysis of $r_\Lambda(l)$ in (24). Recall that $r_\Lambda(l) = \frac{x}{\langle d \rangle} \rho^T_\Lambda(l)$. Since the flow of x is slow, the flow of $r_\Lambda(l)$ for $\Lambda \in [xl, l]$ is controlled by the competition between the growth of $\rho^T_\Lambda(l)$ and $\langle d \rangle$ with Λ. Clearly, the growth of both quantities is due to a monotonic decrease in the total number of blocks N_Λ. But for $\rho^T_\Lambda(l)$, there is an additional mechanism that reduces $\rho^T_\Lambda(l)$. This comes from decimations of T blocks with length l when a rare I block is at cutoff. The rate of these processes is $C^{TI}_\Lambda(l, \Lambda)/\rho^T_\Lambda(l)$. Thus as long as $C^{TI}_\Lambda(l, \Lambda)/\rho^T_\Lambda(l) \ll \rho^T_\Lambda(\Lambda)$, which is the content of assumption 3, this decreasing contribution will be negligible and $r_\Lambda(l)$ will remain approximately constant for $\Lambda \in [xl, l]$. A more precise version of this argument in Appendix B then leads to the key lemma:

Lemma V.3. Under assumptions 1 and 3, along the separatrix we have $r_\Lambda(l) \approx r_l(l)$ up to errors of $O(\log x^{-1} x^c)$ for all $\Lambda \in (xl, l)$ where $c > 0$ and $x = x_\Lambda$. Below the separatrix, the error is strictly smaller, approaching $O(\frac{1}{\mathrm{Superpoly}(\Lambda)})$ in the large Λ limit.

The constancy of $r_\Lambda(l)$ for $\Lambda \in (xl, l)$, combined with the estimates in Lemma V.1, allows us to compute the precise functional form of $\rho^T_\Lambda(l)$ along the critical separatrix. Importantly, $\rho^T_\Lambda(l)$ decays faster than $1/l^2$ everywhere below the separatrix, a property that will be used in the main argument.

Lemma V.4. $\rho^T_\Lambda(l) \approx \frac{x_\Lambda^{-1} \Lambda \log \Lambda}{x_l^{-1} l^2 \log l}$ for $l \in [\Lambda, 2\Lambda + \frac{\Lambda}{x}]$. This in turn implies that $\langle l \rangle \approx \Lambda \log x^{-1}$.

With these technical lemmas in place, we can understand the flow equation for $r_\Lambda(l)$ (24) outside the regime $\Lambda \in [xl, l]$ where the dominant growth mechanism of $\rho^T_\Lambda(l)$ is the production of new T blocks with length l from a $TIT \to T$ move. Following Ref. [48], the strategy is to avoid solving the full

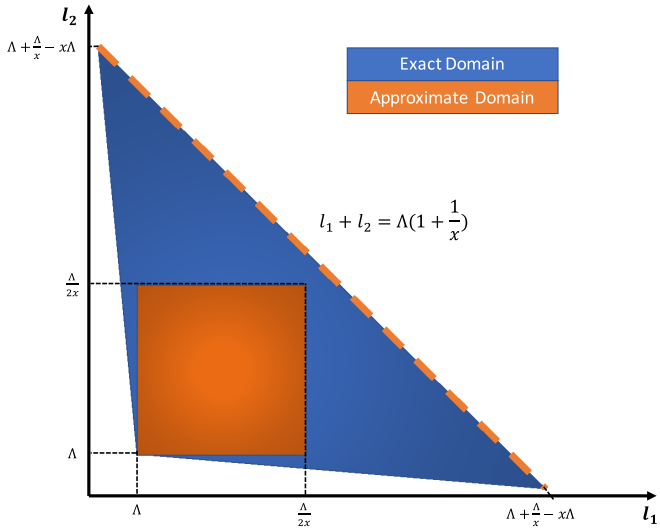

FIG. 6. In this plot we show the exact and approximate integration domains relevant for the production term. The opening angle of the isosceles triangle (exact domain) approaches $\pi/2$ as $x \to 0$.

integro-differential equation but instead derive an approximate recursion relation for $r_\Lambda(\frac{\Lambda}{x})$ in terms of $r_\Lambda(\Lambda)$. For that purpose, we fix $l = \frac{\Lambda}{x}$ and integrate (24) from $\Lambda' = x\Lambda$ to $\Lambda' = \Lambda$. Keeping all terms on the RHS for the moment, we find

$$r_{\Lambda'}(l)\big|_{x\Lambda}^{\Lambda} \approx \int_{x\Lambda}^{\Lambda} \left\{ \left(-\frac{y}{\Lambda'} + \frac{\Lambda' \mu^I_{\Lambda'}(\Lambda')}{\langle d \rangle_{\Lambda'}} - \frac{2C^{TI}_{\Lambda'}(l,\Lambda')}{\rho^T_{\Lambda'}(l)} \right) r_{\Lambda'}(l) + \frac{x}{\langle d \rangle_{\Lambda'}} \int_{\Lambda'}^{l-\Lambda'\frac{1+x}{x}} dl_1 C^{TIT}_{\Lambda'}\left(l_1, \Lambda', l - l_1 - \frac{\Lambda'}{x}\right) \right\}. \tag{29}$$

For notational convenience, we will refer to the first line on the RHS as $F_{\Lambda,\text{depl}}$ and the second line as $F_{\Lambda,\text{prod}}$, in accordance with the general decomposition of flow equations into depletion and production terms. As a sanity check, note that this reduces to the analogous flow equation (15) in Ref. [48] after we plug in the exact solution $\mu^I_\Lambda(d) = \mu^I_\Lambda(\Lambda) e^{-\mu^I_\Lambda(\Lambda)(d-\Lambda)}$ valid for uncorrelated disorder and factorize joint distributions into product of marginals. Now we make a change of variables from $\Lambda' \to l_2 = l - l_1 - \frac{\Lambda'}{x}$ to elucidate the physical picture. Using the slow decay of x, the production term $F_{\Lambda,\text{prod}}$ could be reduced to $x^2 \int_D dl_1 dl_2 \frac{1}{\langle d \rangle_{\Lambda'}} C^{TIT}_{\Lambda'}(l_1, \Lambda', l_2)$ where D is an isosceles triangular integration domain as shown in Fig. 6 and $\Lambda' = \Lambda + 2x(\Lambda - l_1 - l_2)$ depends implicitly on l_1, l_2. Roughly, this term counts all possible ways to form a T block with length l at scale Λ by combining smaller blocks at an earlier stage with cutoff $\Lambda' \in [x\Lambda, \Lambda]$. When $l = \frac{\Lambda}{x}$, in order for the fractal structure of T blocks to be dominant, this term should receive its dominant contributions from $\Lambda' = \Lambda$. Using the fundamental assumptions and Lemma V.3 we can show that this is indeed the case. Moreover, the integral over domain D can be replaced by an integral over an infinite region $[\Lambda, \infty]^2$ up to errors that are suppressed at large Λ if the decay of $C^{TIT}_\Lambda(l_1, \Lambda, l_2)$ with l_1, l_2 is sufficiently fast. This is guaranteed by assumption 3 and the estimate in Lemma V.4.

Finally, since the integral over the infinite region $[\Lambda, \infty]^2$ simply gives $\mu^I_\Lambda(\Lambda)$, we immediately conclude

$$F_{\Lambda,\text{prod}} = \frac{x^2}{\langle d \rangle} \mu^I_\Lambda(\Lambda). \tag{30}$$

Using the decay properties of $\rho^T_\Lambda(l)$, we can also show that $F_{\Lambda,\text{depl}}$ is suppressed relative to $F_{\Lambda,\text{prod}}$, thereby establishing a recursion relation for $r_\Lambda(l)$

$$r_{\Lambda/x}(\Lambda/x) \approx r_\Lambda(\Lambda/x) \approx \frac{x^2}{\langle d \rangle} \mu^I_\Lambda(\Lambda). \tag{31}$$

Using Lemma V.3, we complete the derivation of the projected flow equations in property (3)

$$y_{\Lambda/x} = \frac{\Lambda^2}{x^2} r_{\Lambda/x}(\Lambda/x) \approx \frac{\Lambda^2}{\langle d \rangle} \mu^I_\Lambda(\Lambda) = \left(\frac{y_\Lambda}{x}\right)^2 \langle d \rangle \mu^I_\Lambda(\Lambda). \tag{32}$$

A byproduct of the precise argument in Appendix B is that $\langle d \rangle \mu^I_\Lambda(\Lambda) \sim x \log \Lambda$ at large Λ and along the separatrix. As $x \to 0$, by the assumption of critical slowing down, x scales as a negative power of $\log \Lambda$. Thus $\langle d \rangle \mu^I_\Lambda(\Lambda) \sim x^c$ for some $c < 1$. From this we can simplify the recursion relation as

$$y_{\Lambda/x} \sim \left(\frac{y_\Lambda}{x}\right)^2 x^c \approx \frac{y^2}{x^{2-c}}. \tag{33}$$

This recursion is solved by $y \sim x^\beta$ with $\alpha = 2 - c$. Plugging this back into the exact flow equation (23) for x and introducing the RG time $t = \log \Lambda$, we can get the parametric form of the critical separatrix,

$$\frac{dx}{dt} \approx -x^\beta \quad \to \quad x(t) \sim t^{\frac{1}{c-1}} \quad y(t) \sim t^{\frac{2-c}{c-1}}. \tag{34}$$

When $\langle d \rangle \mu^I_\Lambda(\Lambda) \approx 1$ as in the uncorrelated RG, $c = 0$ and we recover the uncorrelated separatrix $x(t) \sim t^{-1}$, $y \sim t^{-2}$. In the correlated case, it is possible to have $c \neq 0$ so that x, y have different scalings with t. Now let us consider deviations from the critical separatrix $y \approx x^{2-c+\delta_0}$. For δ_0 sufficiently small, $\langle d \rangle \mu^I_\Lambda(\Lambda) \sim x^c$ continues to approximately hold. Thus for every recursion step, $t \to t + \log x^{-1}$,

$$y_{\Lambda/x} \approx \left(\frac{x^{2-c+\delta_0}}{x}\right)^2 x^c \approx x^{2-c+2\delta_0}. \tag{35}$$

The number of RG steps it takes for δ_0 to reach an $O(1)$ value is $\log_2 \delta_0^{-1}$. The elapsed RG time per RG step is $\frac{dt}{dn} = \log x^{-1} \approx \log(\log \Lambda)^{\frac{1}{1-c}} = \frac{1}{1-c} \log t$. This implies that the total RG time T is related to the number of RG steps N as

$$N \approx \int^T \frac{dt}{\frac{dt}{dn}} \approx \frac{(1-c)T}{\log T} \quad \to \quad T \approx \frac{N}{1-c} \log \frac{N}{1-c}. \tag{36}$$

Hence in the limit $\delta_0 \to 0$, the correlation length scales as

$$\xi = e^T \approx \delta_0^{-(1-c)^{-1} \log(\log_2 \delta_0^{-1} (1-c)^{-1})}. \tag{37}$$

As anticipated by the qualitative argument in Sec. V B, the above scaling satisfies $\nu = \infty$. The origin of the double logarithm is an extreme asymmetry between the logarithmic slowdown along the separatrix and the exponential speedup

orthogonal to the separatrix. For any finite value of c, the double logarithmic scaling is robust up to δ_0-independent constants. We have thus established property (3) in Sec. III D.

Finally, to estimate the stretching exponent $\epsilon(x)$ deep in the MBL phase and obtain a more quantitative version of property (1), we have to study the scaling of $\langle d\rangle\mu^I_\Lambda(\Lambda)$. Using the flow equations for $\langle d\rangle$ and $\mu^I_\Lambda(\Lambda)$,

$$\frac{d[\langle d\rangle\mu^I_\Lambda(\Lambda)]}{d\Lambda} \approx -2C^{TI}_{\Lambda,c}(\Lambda,\Lambda)\langle d\rangle + \langle d\rangle\partial_d\mu^I_\Lambda(d)\big|_{d=\Lambda}. \tag{38}$$

By the positivity of C^{TI}_Λ and the numerical observation that $C^{TI}_{\Lambda,c}(\Lambda,\Lambda) < 0$, $0 < -C^{TI}_{\Lambda,c}(\Lambda,\Lambda) < \rho^T_\Lambda(\Lambda)\mu^I_\Lambda(\Lambda)$. Thus we generally have a scaling

$$-2C^{TI}_{\Lambda,c}(\Lambda,\Lambda) \sim \eta\rho^T_\Lambda(\Lambda)\mu^I_\Lambda(\Lambda), \tag{39}$$

where $\eta < 1$ (if $\eta \geqslant 1$, then $\mu^I_\Lambda(\Lambda)$ would flow to ∞ as $\Lambda \to \infty$, which is impossible). This means that

$$\frac{d[\langle d\rangle\mu^I_\Lambda(\Lambda)]}{d\Lambda} \approx \eta\rho^T_\Lambda(\Lambda)[\langle d\rangle\mu^I_\Lambda(\Lambda)], \tag{40}$$

which gives $\log[\langle d\rangle\mu^I_\Lambda(\Lambda)] \approx \eta\int^\Lambda \rho^T_{\Lambda'}(\Lambda')d\Lambda'$ upon integration. On the other hand, close to the MBL fixed line, $\rho^T_\Lambda(\Lambda) \gg \frac{1}{\Lambda}$, and $\log\langle d\rangle \approx \int^\Lambda \rho^T_{\Lambda'}(\Lambda')d\Lambda'$. By definition of y, we therefore conclude that $\log y \approx -\int^\Lambda \rho^T_{\Lambda'}(\Lambda')d\Lambda' +$ subleading. Combining these estimates with the recursion relation, we find

$$-\int^{\Lambda/x} \rho^T_{\Lambda'}(\Lambda')d\Lambda' = (-2+\eta)\int^\Lambda \rho^T_{\Lambda'}(\Lambda')d\Lambda' - 2\log x. \tag{41}$$

Since x freezes to a constant on the MBL fixed line, we can drop $2\log x$ as $\Lambda \to \infty$ in the above equation. The remaining equation is solved by the ansatz

$$\rho^T_\Lambda(\Lambda) \sim \frac{1}{\Lambda^{1-\epsilon}}, \quad -\left(\frac{\Lambda}{x}\right)^\epsilon = (-2+\eta)\Lambda^\epsilon. \tag{42}$$

We now recognize ϵ as the stretching exponent, which must satisfy

$$\epsilon = \frac{\log(2-\eta)}{\log x^{-1}}, \quad 0 \leqslant \eta < 1. \tag{43}$$

Though this result holds for general η, the moment bounds in (14) strongly suggest that $\eta \to 0$ as $\Lambda \to \infty$. Therefore, the expectation is that $\epsilon = \frac{\log 2}{\log x^{-1}}$, which is exactly the uncorrelated value. At this point all three features promised in Sec. III D have been established.

VI. DISCUSSION

In this paper, we have argued via an analytic renormalization group approach that the Morningstar-Huse-Imbrie critical scaling for the MBL transition is not affected by the introduction of spatial correlations in the distribution of initial block parameters. Since our arguments cover correlations with arbitrary wandering exponents, they provide strong evidence that the MHI critical scaling is in fact a robust universality class. Furthermore, many of our arguments continue to apply beyond the MHI context. For hyperuniform correlations, stability holds for asymptotically additive RGs, a broad class that includes all existing phenomenological RGs for the MBL transition. For positive correlations, while the most precise analytic arguments in Sec. V C rely on details of the MHI RG, the more physical arguments in Sec. V A and Sec. V B mostly involve general properties of asymptotically additive avalanche-based RGs. The "factorization" of higher moments in Sec. V A only requires asymptotic additiveness and the vanishing of excess interaction decay rate x at the transition, which is a defining feature of the avalanche mechanism. Likewise, the key ingredients in Sec. V B are that the MBL transition is driven by rare fractal thermal inclusions and the correlation length exponent ν diverges. As pointed out in Ref. [69], both of these features are likely generic for avalanche-based RG schemes including MHI and GVS. Therefore, our arguments suggest that any avalanche-based description of the MBL transition is stable against arbitrary long-range disorder correlations.

Moving forward, there remains a few open questions that need to be addressed. The most important challenge is to go beyond specific RG schemes and develop a scaling theory of the MBL transition from which all critical singularities follow. A first attempt in that direction appeared in Ref. [69], where the avalanche mechanism, combined with an assumption on the analyticity of the β functions, led to the KT universality class on general grounds without invoking specific RG rules. But this conclusion was called into question by the MHI RG, which, despite its simple and well-motivated microscopic rules, featured a nonanalytic β function in the (x, y) plane. Whether such nonanalyticities should be expected in general is a question that can hopefully be settled by improving the arguments of Ref. [69]. An alternative possibility is that analyticity only holds in a higher dimensional parameter space and fails when we project onto the two dimensional subspace spanned by (x, y). The challenge would then be to identify the minimal set of parameters needed for analyticity and constrain the form of the β function in this bigger space using some general physical principles (with quantum avalanche probably playing a key role). Such a framework will obviate the need for more microscopic RG models and provide a much more robust picture of the MBL transition. The effects of long-range disorder correlations on this transition could then be analyzed by adapting the techniques developed in this paper.

Even without a complete scaling theory, it is fruitful to ask within a specific phenomenological RG scheme whether there exists a class of initial disorder correlation that would modify the critical scaling of the uncorrelated random fixed point. One interesting example is quasiperiodic correlation [7,57]. For the symmetric RG of Ref. [25], quasiperiodic initial conditions give rise to a critical exponent $\nu = 1$ [57], which is distinct from the value of ν for the two families of correlations that we have considered (see Appendix C for a more detailed discussion of the symmetric RG), and distinct from the uncorrelated random case. In the MHI RG, the analytic framework that we have developed for hyperuniform and positive correlations does not apply to quasiperiodic correlations which are described by a fixed set of initial block lengths rather than an ensemble. Therefore, although the wandering exponent of quasiperiodic correlation $w = 0$ coincides with that of hyperuniform correlation with $\alpha = 1$, we cannot con-

clude that $\nu = \infty$ for the quasiperiodic case. Understanding the fate of the quasiperiodic MBL transition will likely require new analytic insights.

Finally, we should remark that the moment bounds of joint distributions $C_\Lambda^{TI\cdots T}$ in block RGs and the BBGKY hierarchy of correlated flows developed in this paper may have applications to more general functional RGs. One topic where the formalism might be helpful is the generalized Harris bound/correlated CCFS bound that we discussed in the introduction.

ACKNOWLEDGMENTS

We thank U. Agrawal, D. Huse, A. Morningstar, H. Singh, M. Serbyn, and B. Ware for useful discussions and collaboration on related works. We also thank Yunkun Zhou for helpful comments on bounding probability distributions. We acknowledge support from NSF Grants No. DMR-2103938 (S.G.), No. DMR-2104141 (R.V.), the US Department of Energy, Office of Science, Basic Energy Sciences, under Early Career Award No. DE-SC0021111 (V.K.), the Alfred P. Sloan Foundation through Sloan Research Fellowships (V.K. and R.V.), and the Packard Fellowship in Science and Engineering (V.K.). Some of the computing for this project was performed on the Sherlock cluster. We would like to thank Stanford University and the Stanford Research Computing Center for providing computational resources and support that contributed to these research results.

APPENDIX A: DERIVATION OF CORRELATED FLOW EQUATIONS

Spatial correlations in the initial T/I-block lengths force us to consider a functional RG of the joint probability distribution $P_\Lambda(\vec{l}^I, \vec{l}^T)$ instead of the single-block marginals $\rho_\Lambda^T(l^T)$, $\mu_\Lambda^I(d)$ studied in Ref. [48]. However, to understand the behavior of the order parameters x_Λ, y_Λ, which depend only on single-block marginals and their integrals, we do not need to keep track of the fine-grained renormalization of $P_\Lambda(\vec{l}^T, \vec{l}^I)$. Instead, we will develop a hierarchy of equations (analogous to the BBGKY hierarchy is classical statistical mechanics), where the marginal distribution of n nearest neighbors depends on the distribution of $n+2$ nearest neighbors (see Refs. [71–75] for original papers on the BBGKY hierarchy). This set of equations do not close at any finite order but will be sufficient for a precise analysis of the near-critical regime.

The general structure of the flow equations can be understood via the following schematic equation:

$$\partial_\Lambda C_\Lambda^{(n)}(l_1, d_1, \ldots) = F_{\text{depl}}\big[C_\Lambda^{(n+2)}\big] + F_{\text{prod}}\big[C_\Lambda^{(n+2)}\big]. \quad \text{(A1)}$$

Here, $C_\Lambda^{(n)}(l_1, d_1, \ldots)$ is the probability that a contiguous chain of n blocks have lengths $(l_1, d_1, \ldots)$ when the length cutoff is Λ. The flow of $C_\Lambda^{(n)}$ has two contributions: F_{depl} is a depletion term that accounts for RG moves where a chain of n blocks with length $(l_1, d_1, \ldots)$ at cutoff Λ are destroyed when we move the cutoff $\Lambda + d\Lambda$; in contrast, F_{prod} is a production term that encodes RG moves that create a new chain of n blocks with lengths $(l_1, d_1, \ldots)$, which was not present at cutoff Λ. To be concrete, we consider the case where n = 1, so that the LHS is just a single-block marginal. For T and I blocks we have

$$\begin{aligned}\partial_\Lambda \rho_\Lambda^T(l) &= \rho_\Lambda^T(l)\big[\mu_\Lambda^I(\Lambda) + \rho_\Lambda^T(\Lambda)\big] - 2C_\Lambda^{TI}(l, \Lambda) \\ &\quad + \int_\Lambda^{l-\frac{\Lambda}{x}-\Lambda} C_{\Lambda,c}^{TIT}\left(l_1, \Lambda, l - \frac{\Lambda}{x} - l_1\right) dl_1, \quad \text{(A2)} \\ \partial_\Lambda \mu_\Lambda^I(d) &= \mu_\Lambda^I(d)\big[\mu_\Lambda^I(\Lambda) + \rho_\Lambda^T(\Lambda)\big] - 2C_\Lambda^{TI}(\Lambda, d) \\ &\quad + \int_\Lambda^d C_\Lambda^{ITI}(s, \Lambda, d + \Lambda - s) ds. \quad \text{(A3)}\end{aligned}$$

In each of the flow equations above, the first and second lines are depletion and production terms respectively. In the uncorrelated limit, the multiblock correlations factorize as products of single-block marginals $C^{TI}(l, d) = \rho_\Lambda^T(l)\mu_\Lambda^I(d)$, $C^{TIT}(l_1, d, l_2) = \rho^T(l_1)\mu^I(d)\rho^T(l_2)$ etc., and the resulting flow equations agree with those obtained in Ref. [48]. Following the same procedure, it is conceptually simple to derive the full hierarchy of equations. For clarity, we will only present the next simplest equation in the hierarchy (which turns out to be all we need near criticality). This flow equation will involve two types of contributions: one coming from the depletion of thermal blocks with length l_1, l_2 that have already been produced in earlier stages in the RG (i.e., at cutoff smaller than Λ) and the other coming from the production of thermal blocks with length l_1, l_2 due to decimation of I blocks with $d = \Lambda$. Taking both contributions into account, the number density flows as

$$\begin{aligned}n_{\Lambda+d\Lambda}^{TIT}(l_1, \Lambda + d\Lambda, l_2) &= n_\Lambda^{TIT}(l_1, \Lambda, l_2) + d\Lambda\Bigg[-C_\Lambda^{ITIT}(\Lambda, l_1, d, l_2) - C_\Lambda^{TITI}(l_1, d, l_2, \Lambda) \\ &\quad + \int_\Lambda^\infty d\tilde{l}_1 C_\Lambda^{TITIT}\left(\tilde{l}_1, \Lambda, l_1 - \frac{\Lambda}{x} - \tilde{l}_1, d, l_2\right) + \int_\Lambda^\infty d\tilde{l}_1 C_\Lambda^{TITIT}\left(l_1, d, \tilde{l}_2, \Lambda, l_2 - \frac{\Lambda}{x} - \tilde{l}_2\right)\Bigg] \\ &\quad + \int_\Lambda^\infty ds C_\Lambda^{TITIT}(l_1, s, \Lambda, d + \Lambda - s, l_2)\Bigg]. \quad \text{(A4)}\end{aligned}$$

Let the total number of I blocks be N_Λ (which is equal to the number of T blocks) with flow equation $N_{\Lambda+d\Lambda} = N_\Lambda[1 - d\Lambda(\rho_\Lambda^T(\Lambda) + \mu_\Lambda^I(\Lambda)]$. Dividing both sides of the previous equation by $N_{\Lambda+d\Lambda}$ and recalling the definition $n_\Lambda^{TIT}/N_\Lambda = C_\Lambda^{TIT}$, we get

$$\partial_\Lambda C_\Lambda^{TIT}(l_1, d, l_2) = F_{\text{depl}} + F_{\text{prod}}, \quad \text{(A5)}$$

where the depletion and production terms are given by

$$F_{\text{depl}} = C_\Lambda^{TIT}(l_1, d, l_2)[\rho_\Lambda^T(\Lambda) + \mu_\Lambda^I(\Lambda)] - C_\Lambda^{ITIT}(\Lambda, l_1, d, l_2) - C_\Lambda^{TITI}(l_1, d, l_2, \Lambda), \tag{A6}$$

$$F_{\text{prod}} = \int_\Lambda^\infty ds\left[C_\Lambda^{TITIT}\left(s, \Lambda, l_1 - \frac{\Lambda}{x} - s, d, l_2\right) + C_\Lambda^{TITIT}\left(l_1, d, s, \Lambda, l_2 - \frac{\Lambda}{x} - s\right) + C_\Lambda^{TITIT}(l_1, s, \Lambda, d + \Lambda - s, l_2)\right]. \tag{A7}$$

The two-parameter RG flows that we are interested in depend not on the full distribution but rather on the moments of these distributions. It is easy to derive flow equations for the moments from the full PDEs above. We enumerate a full set of these equations here:

$$\frac{d\langle l^I\rangle}{d\Lambda} = \mu_\Lambda^I(\Lambda)\left[\langle l^I\rangle - \frac{\Lambda}{x}\right] + \rho_\Lambda^T(\Lambda)[\langle l^I\rangle + \Lambda], \tag{A8}$$

$$\frac{d\langle l^T\rangle}{d\Lambda} = \rho_\Lambda^T(\Lambda)[\langle l^T\rangle - \Lambda] + \mu_\Lambda^I(\Lambda)\left[\langle l^T\rangle + \frac{\Lambda}{x}\right], \tag{A9}$$

$$\frac{d\langle d\rangle}{d\Lambda} = \left[\mu_\Lambda^I(\Lambda) + \rho_\Lambda^T(\Lambda)\right](\langle d\rangle - \Lambda). \tag{A10}$$

Note that these equations are equivalent in form to their uncorrelated analogues in Ref. [29]. However, since $\rho_\Lambda^T(\Lambda)$, $\mu_\Lambda^I(\Lambda)$ are shifted by correlations, the functional dependence of $\langle d\rangle$, $\langle l^I\rangle$, $\langle l^T\rangle$ on Λ may also be different from the uncorrelated RG.

The proof of these three formulas are structurally identical and rather tedious, so we will only give the simplest version of the calculation. Consider $\langle d\rangle = \int_\Lambda^\infty dd\mu_\Lambda^I(d)\cdot d$. A few simple algebraic manipulations lead to

$$\begin{aligned}
\frac{d}{d\Lambda}\langle d\rangle &= -\mu_\Lambda^I(\Lambda)\Lambda + \int_\Lambda^\infty \partial_\Lambda\mu_\Lambda^I(d)\cdot d \\
&= -\mu_\Lambda^I(\Lambda)\Lambda + \int_\Lambda^\infty \mu_\Lambda^I(d)\left[\mu_\Lambda^I(\Lambda) + \rho_\Lambda^T(\Lambda)\right]d - 2\int_\Lambda^\infty C_\Lambda^{TI}(\Lambda, d)d + \int_\Lambda^\infty dd\int_\Lambda^d dx C_\Lambda^{ITI}(d - x + \Lambda, \Lambda, x)d \\
&= -\mu_\Lambda^I(\Lambda)\Lambda + \langle d\rangle\left[\mu_\Lambda^I(\Lambda) + \rho_\Lambda^T(\Lambda)\right] - 2\langle d_i|l_i^T = \Lambda\rangle + \int_\Lambda^\infty dx\int_\Lambda^\infty dy\int dd\delta(d - x + \Lambda - y)C_\Lambda^{ITI}(y, \Lambda, x)d \\
&= -\mu_\Lambda^I(\Lambda)\Lambda + \langle d\rangle\left[\mu_\Lambda^I(\Lambda) + \rho_\Lambda^T(\Lambda)\right] - 2\langle d_i|l_i^T = \Lambda\rangle + 2\langle d_i|l_i^T = \Lambda\rangle - \Lambda\rho_\Lambda^T(\Lambda) \\
&= \left[\mu_\Lambda^I(\Lambda) + \rho_\Lambda^T(\Lambda)\right](\langle d\rangle - \Lambda).
\end{aligned} \tag{A11}$$

where in the third line we introduced the conditional expectation value $\langle\cdot|\cdot\rangle$ and in the fourth line we used the following facts that follow from definition:

$$\begin{aligned}
\int C_\Lambda^{ITI}(x, l, y)dy &= C_\Lambda^{TI}(l, x) \\
\int C_\Lambda^{ITI}(x, l, y)dx &= C_\Lambda^{TI}(l, y) \\
\int C_\Lambda^{ITI}(x, l, y)dxdy &= \rho_\Lambda^T(l).
\end{aligned} \tag{A12}$$

This completes the proof of Lemma V.1.

APPENDIX B: DERIVATION OF RECURSION RELATION FOR CORRELATED MHI RG

In the main text, we outlined an argument for the stability of MBL criticality in the MHI RG. In this Appendix, we will fill in some of the technical details. Recall the fundamental variables in our RG,

$$x_\Lambda = \frac{\langle d\rangle}{\langle l^I\rangle}, \quad r_\Lambda(l) = \frac{x}{\langle d\rangle}\rho_\Lambda^T(l), \quad y = r_\Lambda(\Lambda)\Lambda^2. \tag{B1}$$

In Sec. V C, we already derived the exact flow equation $\frac{dx}{d\Lambda} = -\frac{(1+x)y}{\Lambda}$ for x_Λ. Here we will derive the flow equation for $r_\Lambda(l)$, which will facilitate our analysis of y later. Differentiating the definition directly and using the exact flow equation for x, we get three terms, which partially cancel each other,

$$\begin{aligned}
\partial_\Lambda r_\Lambda(l) &= \frac{dx}{d\Lambda}\frac{\rho_\Lambda^T(l)}{\langle d\rangle} - \frac{x}{\langle d\rangle^2}\rho_\Lambda^T(l)\partial_\Lambda\langle d\rangle + \frac{x}{\langle d\rangle}\partial_\Lambda\rho_\Lambda^T(l) \\
&= \frac{1}{x}\frac{dx}{d\Lambda}r_\Lambda(l) - \frac{\langle d\rangle - \Lambda}{\langle d\rangle}\left[\mu_\Lambda^I(\Lambda) + \rho_\Lambda^T(\Lambda)\right]r_\Lambda(l)
\end{aligned}$$

$$+\frac{x}{\langle d\rangle}\left\{\rho^T_\Lambda(l)\big[\mu^I_\Lambda(\Lambda)+\rho^T_\Lambda(\Lambda)\big]-2C^{TI}_\Lambda(l,\Lambda)+\int_\Lambda^{l-\Lambda(1+x^{-1})} C^{TIT}_\Lambda\left(l_1,\Lambda,l-\frac{\Lambda}{x}-l_1\right)dl_1\right\}$$
$$=\left(-\frac{y}{\Lambda}+\frac{\Lambda\mu^I_\Lambda(\Lambda)}{\langle d\rangle}-\frac{2C^{TI}_\Lambda(l,\Lambda)}{\rho^T_\Lambda(l)}\right)r_\Lambda(l)+\frac{x}{\langle d\rangle}\int_\Lambda^{l-\Lambda(1+x^{-1})} C^{TIT}_\Lambda\left(l_1,\Lambda,l-\frac{\Lambda}{x}-l_1\right)dl_1. \tag{B2}$$

Integrating the above equation from $x\Lambda$ to Λ gives equation (29) in the main text, which we rewrite below

$$r_{\Lambda'}(l)\big|^{\Lambda}_{x\Lambda}\approx\int_{x\Lambda}^{\Lambda}\left\{\left(-\frac{y}{\Lambda'}+\frac{\Lambda'\mu^I_{\Lambda'}(\Lambda')}{\langle d\rangle_{\Lambda'}}-\frac{2C^{TI}_{\Lambda'}(l,\Lambda')}{\rho^T_{\Lambda'}(l)}\right)r_{\Lambda'}(l)+\frac{x}{\langle d\rangle}\int_{\Lambda'}^{l-\Lambda'(1+x^{-1})} C^{TIT}_{\Lambda'}\left(l_1,\Lambda',l-\frac{\Lambda'}{x}-l_1\right)dl_1\right\}. \tag{B3}$$

As explained in the main text, our goal is to show that the second term dominates over the other two terms. To do that, we first recall the "fundamental assumptions" that go into our analysis:

Assumption 1: Critical slowing down holds along the separatrix so that $x\sim t^{-\alpha}$ for some positive exponent α where $t=\log\Lambda$ is the RG time. In the uncorrelated MHI RG, $\alpha=1$. Here we only assume that α is finite.

Assumption 2: Along and below the critical separatrix, as the I blocks become much longer than the T blocks, the distribution of deficit lengths $\mu^I_\Lambda(d)$ for I blocks tends to become wider and flatter. Concretely, we will assume that $\mu^I_\Lambda(\Lambda)$ decreases with Λ and the derivative $\partial_d\mu^I_\Lambda(d)$ evaluated at the cutoff $d=\Lambda$ goes to zero sufficiently rapidly as $\Lambda\to\infty$,

$$-\partial_d\log\mu^I_\Lambda(d),\ -\partial_d\log C^{TIT}_\Lambda(l_1,d,l_2)\big|_{d=\Lambda}\ll\rho^T_{\Lambda,\mathrm{crit}}(\Lambda) \tag{B4}$$

Assumption 3: The connected distributions of nearest-neighbor T and I blocks are upper bounded by a function that is much larger than the product of marginal distributions for $l\in[\Lambda,\Lambda/x]$,

$$\left|\frac{C^{TI}_{\Lambda,c}(l,\Lambda)}{\rho^T_\Lambda(l)\mu^I_\Lambda(\Lambda)}\right|,\ \left|\frac{C^{TITI}_{\Lambda,c}(l_1,\Lambda,l_2,\Lambda)}{C^{TIT}_\Lambda(l_1,\Lambda,l_2)\mu^I_\Lambda(\Lambda)}\right|\ll\frac{\rho^T_{\Lambda,\mathrm{crit}}(\Lambda)}{\mu^I_\Lambda(\Lambda)}. \tag{B5}$$

where $\ll$ means a multiplicative factor that is $\frac{1}{Poly(t)}$ and hence only logarithmically small in $\log\Lambda$.

The motivation and numerical tests for these assumptions are discussed in the main text and will not be repeated here. With these assumptions in mind, we continue the analysis of (B3). We denote the first term on the RHS of (B3) by $F_{\Lambda,\mathrm{depl}}$ since it captures the depletion of T blocks that have been produced at an earlier RG time. The second term, which captures the production of new T blocks will be denoted by $F_{\Lambda,\mathrm{prod}}$. As a general observation, note that the various terms in $F_{\Lambda,\mathrm{depl}}, F_{\Lambda,\mathrm{prod}}$ correspond to various levels of the hierarchy: from the lowest level moments $\langle\ldots\rangle$ to the highest level three-block joint distributions. The flow equations are a bridge between low and high levels in the hierarchy. The general structure of the two-parameter phase diagram gives us important information about low levels in the hierarchy, for example the relationship between various moments $\langle l^T\rangle, \langle l^I\rangle, \langle d\rangle$. So our general strategy is to bootstrap the higher level distributions from the low level information via the flow equations.

Lemma B.1. Under assumption 1, $\langle d\rangle\sim\Lambda\log\Lambda\gg\Lambda$, $\mu^I_\Lambda(\Lambda)<x\rho^T_\Lambda(\Lambda)$, $\rho^T_\Lambda\approx\frac{1}{\Lambda}+O(\frac{1}{\Lambda\mathrm{Poly}(\log\Lambda)})$ in the large Λ limit along the critical separatrix. Below the critical separatrix (in the MBL phase), $\langle d\rangle\gg\Lambda$ and $\mu^I_\Lambda(\Lambda)<x\rho^T_\Lambda(\Lambda)$ still hold.

Proof. We begin by showing that $\langle d\rangle\gg\Lambda$ without fixing its precise scaling. Suppose that $\langle d\rangle\gg\Lambda$ does not hold, then since $\langle d\rangle>\Lambda$, there must be a finite $k\geqslant 1$ such that $\langle d\rangle\sim k\Lambda+$ subleading at large Λ. The flow equation for $\langle d\rangle$ thus reduces to

$$k=\frac{d\langle d\rangle}{d\Lambda}=\big[\rho^T_\Lambda(\Lambda)+\mu^I_\Lambda(\Lambda)\big](\langle d\rangle-\Lambda)$$
$$=\big[\rho^T_\Lambda(\Lambda)+\mu^I_\Lambda(\Lambda)\big][(k-1)\Lambda+o(\Lambda)] \tag{B6}$$

If $k>1$, then to leading order in Λ, $\mu^I_\Lambda(\Lambda)+\rho^T_\Lambda(\Lambda)\approx\frac{k}{k-1}\frac{1}{\Lambda}$. By combining the flow equation for $\langle l^I\rangle$ and $\langle l^T\rangle$, we immediately see that $\langle l^I\rangle+\langle l^T\rangle\sim\Lambda^{1+\frac{1}{k-1}}$. As argued in the main text (and suggested by numerics) the thermal fraction flows to zero along the critical separatrix, implying that $\langle l^I\rangle>\langle l^T\rangle$. This forces the scaling $\langle l^I\rangle\sim\Lambda^{1+\frac{1}{k-1}}$ and hence $x\sim\Lambda^{-\frac{1}{k-1}}$. For any $k>1$, this is an exponentially fast decay in the RG time $t=\log\Lambda$, violating assumption 1. If $k=1$, then $\mu^I_\Lambda(\Lambda)+\rho^T_\Lambda(\Lambda)\approx\frac{1}{o(\Lambda)}$, which implies that $\langle l^I\rangle+\langle l^T\rangle$ grows faster than any power law in Λ and x decays faster than any power law in Λ. This leads to an even stronger violation of assumption 1. Hence, we conclude that $\langle d\rangle\gg\Lambda$.

To learn something about $\mu^I_\Lambda(\Lambda), \rho^T_\Lambda(\Lambda)$, we go back to the flow equation for $\langle l^I\rangle, \langle l^T\rangle$. Since $\langle l^T\rangle/\langle l^I\rangle\to 0$ "along and below" the critical separatrix, we must demand that $\frac{d\log f}{d\Lambda}$ be a monotonically decreasing function at large Λ where f is the thermal fraction. Using the flow equation for $\langle l^T\rangle, \langle l^I\rangle$, it is easy to see that

$$\frac{d\log f}{d\Lambda}=\frac{\Lambda}{\langle l^T\rangle}\left[\frac{\mu^I_\Lambda(\Lambda)}{x}-\rho^T_\Lambda(\Lambda)\right]. \tag{B7}$$

In order for the RHS to be negative, we must have $\mu^I_\Lambda(\Lambda)<x\rho^T_\Lambda(\Lambda)$ as claimed in the lemma.

To further fix the precise scaling of $\rho^T_\Lambda(\Lambda)$ and $\langle d\rangle$, we go back to the flow equation for x,

$$\frac{dx}{d\Lambda}=-\frac{\Lambda^2 x}{\Lambda\langle d\rangle}\rho^T_\Lambda(\Lambda)=-\frac{\Lambda x\rho^T_\Lambda(\Lambda)}{\langle d\rangle}\quad\to\quad\frac{d\log x}{d\log\Lambda}$$
$$=-\frac{\Lambda^2\rho^T_\Lambda(\Lambda)}{\langle d\rangle}. \tag{B8}$$

In the large Λ limit, we have already shown that $\rho^T_\Lambda(\Lambda)\gg\mu^I_\Lambda(\Lambda)$ and $\langle d\rangle\gg\Lambda$. Therefore, the flow equation for $\langle d\rangle$ reduces to $\frac{d\langle d\rangle}{d\Lambda}=[\rho^T_\Lambda(\Lambda)+\mathrm{subleading}](\langle d\rangle-\Lambda)$. We now

do a simple case work. If $\lim_{\Lambda\to\infty}\Lambda\rho^T_\Lambda(\Lambda)>1$, then $\langle d\rangle$ grows at least as fast as $\Lambda^{1+\epsilon}$ for some $\epsilon>0$. This would mean $\frac{d\log x}{d\log\Lambda}\sim-\frac{1}{\Lambda^\epsilon}$, which implies that $x\sim\frac{1}{\mathrm{Poly}(\Lambda)}$, leading to a contradiction. On the other hand, if $\lim_{\Lambda\to\infty}\Lambda\rho^T_\Lambda(\Lambda)<\frac{1}{\Lambda}$, then $\langle d\rangle=o(\Lambda)$, violating the constraint that $\langle d\rangle>\Lambda$. Hence, we conclude that $\rho^T_\Lambda(\Lambda)\approx\frac{1}{\Lambda}+\text{subleading}$. To get the scaling of the subleading terms, we return again to the flow equation for x. By assumption, x decays as a polynomial in the RG time $\log\Lambda$. This implies that $\frac{dx}{d\Lambda}\sim-\frac{x}{\Lambda\log\Lambda}$, which, together with the leading-order scaling of $\rho^T_\Lambda(\Lambda)$, forces $\langle d\rangle\sim\Lambda\log\Lambda$. In order for this scaling to be consistent with $\rho^T_\Lambda(\Lambda)\approx\frac{1}{\Lambda}$, $\mu^I_\Lambda(\Lambda)<x\rho^T_\Lambda$ and the exact flow equation $\frac{d\langle d\rangle}{d\Lambda}=[\rho^T_\Lambda(\Lambda)+\mu^I_\Lambda(\Lambda)](\langle d\rangle-\Lambda)$, we must demand $\rho^T_\Lambda(\Lambda)+\mu^I_\Lambda(\Lambda)\approx\frac{1}{\Lambda}+o(\frac{1}{\Lambda\log\Lambda})$. Independent of the precise scaling of x with Λ, we therefore conclude that $\rho^T_\Lambda(\Lambda)\approx\frac{1}{\Lambda}+O(\frac{1}{\Lambda\mathrm{Poly}(\log\Lambda)})$. This concludes the proof of estimates along the separatrix.

Below the separatrix, $\rho^T_\Lambda(\Lambda)>\frac{1}{\Lambda}$ because T blocks become even likely to be decimated. This means that $\langle d\rangle\sim e^{\int^\Lambda\rho^T_{\Lambda'}(\Lambda')d\Lambda'}$ grows faster than along the separatrix and hence faster than Λ. This concludes the second part of the Lemma. ■

Lemma B.2. Under assumptions 1 and 3, along the separatrix we have $r_\Lambda(l)\approx r_l(l)$ up to errors of $O(\log x^{-1}x^c)$ for all $\Lambda\in(xl,l)$ where $c>0$ and $x=x_\Lambda$. Below the separatrix, the error is strictly smaller, approaching $O(\frac{1}{\mathrm{Superpoly}(\Lambda)})$ in the large Λ limit.

Proof. In the flow equation (24), production terms give zero contribution whenever $\Lambda\in(xl,l)$ because the shortest T block created from a $TIT\to T$ move at cutoff Λ has length greater than or equal to $\frac{\Lambda}{x}$. Hence we may focus only on the depletion term

$$\partial_\Lambda r_\Lambda(l)=\left(-\frac{y}{\Lambda}+\frac{\Lambda\mu^I_\Lambda(\Lambda)}{\langle d\rangle}-\frac{2C^{TI}_\Lambda(l,\Lambda)}{\rho^T_\Lambda(l)}\right)r_\Lambda(l)$$
$$\to\quad r_{\Lambda_2}(l)=e^{\int_{\Lambda_1}^{\Lambda_2}\left(-\frac{y}{\Lambda}+\frac{\Lambda\mu^I_\Lambda(\Lambda)}{\langle d\rangle}-\frac{2C^{TI}_\Lambda(l,\Lambda)}{\rho^T_\Lambda(l)}\right)d\Lambda}r_{\Lambda_1}(l). \tag{B9}$$

We first work along the separatrix. At large Λ, $y=\frac{x}{\langle d\rangle}\rho^T_\Lambda(\Lambda)\Lambda^2\sim\frac{x\Lambda}{\langle d\rangle}$. Since $x\ll1$, $\frac{y}{\Lambda}=\frac{x}{\langle d\rangle}\sim\frac{x}{\Lambda\log\Lambda}$. Similarly, as $\mu^I_\Lambda(\Lambda)\approx\frac{x}{\Lambda}$, the second term $\frac{\Lambda\mu^I_\Lambda(\Lambda)}{\langle d\rangle}\approx\frac{x}{\langle d\rangle}\approx\frac{x}{\Lambda\log\Lambda}$. Finally, by assumption 3, $C^{TI}_\Lambda(l,\Lambda)/\rho^T_\Lambda(l)\ll\rho^T_\Lambda(\Lambda)\sim\frac{1}{\Lambda}$. Here $\ll$ means a multiplicative factor that is a negative power of the RG time $t=\log\Lambda$. By the assumption of critical slowing down, this can also be formulated as a factor x^c for some $c>0$.

$$\int_{xl}^{l}\left(-\frac{y}{\Lambda}+\frac{\Lambda\mu^I_\Lambda(\Lambda)}{\langle d\rangle}-\frac{2C^{TI}_\Lambda(l,\Lambda)}{\rho^T_\Lambda(l)}\right)d\Lambda$$
$$\lesssim\int_{\log(xl)}^{\log l}d(\log\Lambda)x^c\approx\log x^{-1}x^c. \tag{B10}$$

Along the separatrix, $x\to0$ at large Λ. Therefore, for sufficiently large Λ, we have

$$r_l(l)\approx e^{-\log x^{-1}x^c}r_\Lambda(l)\approx(1-\log x^{-1}x^c)r_\Lambda(l). \tag{B11}$$

implying that $r_l(l)$, $r_{xl}(l)$ are equal up to small corrections. Since $r_\Lambda(l)$ decreases monotonically from $\Lambda=xl$ to l, it must in fact be true that $r_l(l)\approx r_\Lambda(l)$ for all $\Lambda\in(xl,l)$, which is what we set out to prove.

Below the separatrix, we can reexamine the scaling of all three terms. As the flow deviates from the separatrix and tends towards the MBL fixed line, y and $\mu^I_\Lambda(\Lambda)$ decay to 0 faster, while $\langle d\rangle$ grows to ∞ faster as Λ increases, since the decimation rate of T blocks increases monotonically. This trend makes all three terms decay faster towards 0. Hence we still have $r_l(l)\approx r_\Lambda(l)$ for all $\Lambda\in(xl,l)$. For very large Λ, $\rho^T_\Lambda(\Lambda)$ will settle into some asymptotic scaling with Λ such that $\rho^T_\Lambda(\Lambda)\gg O(\frac{1}{\Lambda})$. This implies that $\langle d\rangle,y\sim e^{\int^\Lambda\rho^T_{\Lambda'}(\Lambda')}\sim\mathrm{Superpoly}(\Lambda)$. Hence, the asymptotic error rate is

$$r_l(l)\approx r_\Lambda(l)+O\left(\frac{1}{\mathrm{Superpoly}(\Lambda)}\right), \tag{B12}$$

as we set out to show. ■

Lemma B.3. The following more concrete estimates about the distribution of T-block lengths hold along the separatrix: $\rho^T_\Lambda(l)\approx\frac{x_\Lambda^{-1}\Lambda\log\Lambda}{x_l^{-1}l^2\log l}$ for $l\in[\Lambda,2\Lambda+\frac{\Lambda}{x}]$. This in turn implies that $\langle l\rangle\approx\Lambda\log x^{-1}$.

Proof. From Lemma B.2, we know that for $l\in[\Lambda,\frac{\Lambda}{x}+2\Lambda]$,

$$r_l(l)\approx r_\Lambda(l)\quad r_\Lambda(l)=\frac{x_\Lambda}{\langle d\rangle(\Lambda)}\rho^T_\Lambda(l). \tag{B13}$$

Using the scaling estimates for $\langle d\rangle(\Lambda)$, $\rho^T_\Lambda(\Lambda)$ and assumption 1, we can immediate prove the estimate for $\rho^T_\Lambda(l)$,

$$\frac{x_l}{l\log l}\frac{1}{l}\approx\frac{x_\Lambda}{\Lambda\log\Lambda}\rho^T_\Lambda(l)\quad\to\quad\rho^T_\Lambda(l)\approx\frac{x_\Lambda^{-1}\Lambda\log\Lambda}{x_l^{-1}l^2\log l}. \tag{B14}$$

Using this formula, we can estimate the average T-block length,

$$\langle l\rangle\approx\int_\Lambda^{\Lambda/x}\frac{x_\Lambda^{-1}\Lambda\log\Lambda}{x_l^{-1}l^2\log l}ldl$$
$$\approx x_\Lambda^{-1}\Lambda\log\Lambda\int_{\log\Lambda}^{\log\Lambda+\log x^{-1}}\frac{1}{x_l^{-1}\log l}d(\log l). \tag{B15}$$

By assumption 1 again, $x_\Lambda^{-1}=\mathrm{Poly}(\log\Lambda)$. This immediately implies that

$$\langle l\rangle\approx\frac{\Lambda\log\Lambda x_\Lambda^{-1}}{x_\Lambda^{-1}\log\Lambda}\log x^{-1}\approx\Lambda\log x^{-1}, \tag{B16}$$

which is what we set out to show. ■

Using the estimates for $\rho^T_\Lambda(\Lambda)$, we can obtain some more precise control over $\mu^I_\Lambda(\Lambda)$ and x:

Corollary B.4. Under assumptions 1 and 3 and along the separatrix, $\mu^I_\Lambda(\Lambda)/x\approx\rho^T_\Lambda(\Lambda)+O(\frac{1}{\Lambda\log\Lambda})$.

Proof. By assumptions 1 and 3, the previous two lemmas hold and we have $\mu^I_\Lambda(\Lambda)<x\rho^T_\Lambda(\Lambda)$. Here, we want to show that they are in fact equal to leading order in Λ. For that we return to the flow equation for the thermal fraction $f=\frac{\langle l^T\rangle}{\langle l^I\rangle+\langle l^T\rangle}$ (for notational clarity we use $\langle l^T\rangle$ instead of $\langle l\rangle$ to denote the average T-block length in this proof). Along the critical separatrix, we have $\langle l^T\rangle=\Lambda f_T(\Lambda)$, $\langle l^I\rangle=\Lambda f_I(\Lambda)$

where $f_T(\Lambda) \sim \log x^{-1}$ and $f_I(\Lambda) \sim \frac{\log \Lambda}{x}$ as we flow towards the fixed point at $f = 0$. Now the flow equation for f dictates that

$$\frac{d \log f}{d \log \Lambda} \approx -\frac{\Lambda^2}{\langle l^T \rangle}[-\mu^I_\Lambda(\Lambda)/x + \rho^T_\Lambda(\Lambda)]. \tag{B17}$$

Now let us evaluate the LHS approximately,

$$\begin{aligned}\frac{d \log f}{d \log \Lambda} &= \frac{d \log f_T(\Lambda)}{d \log \Lambda} - \frac{d \log[f_T(\Lambda) + f_I(\Lambda)]}{d \log \Lambda} \\ &\approx -\frac{d \log f_I(\Lambda)}{d \log \Lambda} + \text{subleading},\end{aligned} \tag{B18}$$

where in the last step we used the fact that $f_I(\Lambda)$ grows much faster than $f_T(\Lambda)$ at large Λ. This estimate implies that

$$\frac{d \log f_I(\Lambda)}{d \log \Lambda} \approx O\left(\frac{\Lambda[-\mu^I_\Lambda(\Lambda)/x + \rho^T_\Lambda(\Lambda)]}{\log x^{-1}}\right). \tag{B19}$$

But if $f_I(\Lambda) \sim \log \Lambda/x$, $\frac{d \log f_I(\Lambda)}{d \log \Lambda} = O(\frac{1}{\log \Lambda})$. Since $\log x^{-1}$ is smaller than any polynomial in $\log \Lambda$, the equation above is inconsistent unless $\mu^I_\Lambda(\Lambda)/x - \rho^T_\Lambda(\Lambda) = O(\frac{1}{\Lambda \log \Lambda})$.

These lemmas already allow us to study the relationship between x, y strictly along the separatrix. But since we are interested in the entire region below the separatrix, we need to give a more precise argument for how the RHS of (B3) scales. In step (1), we obtain a compact formula for $F_{\Lambda,\text{prod}}$ valid in the large Λ limit. In step (2) we argue that $F_{\Lambda,\text{depl}}$ is suppressed relative to $F_{\Lambda,\text{prod}}$, thereby establishing the recursion relation for $r_\Lambda(l)$ and hence for $y = r_\Lambda(\Lambda)\Lambda^2$.

As a preface to the remaining arguments, we emphasize that the logic above is a direct generalization of the logic for uncorrelated MHI explained in Ref. [48]. In the uncorrelated case, step (1) requires a careful analysis of the decay properties of the integrand $\rho^T_{\Lambda'}(l_1)\mu^I_{\Lambda'}(\Lambda')\rho^T_{\Lambda'}(l - \Lambda'/x - l_1)$ in the integration domain Fig. 6. For the correlated case, the integration domain does not change, but the integrand no longer factorizes. Thus the main challenge is to use the lemmas and fundamental assumptions to argue for similar decay properties. Step (2) in the uncorrelated case is a direct application of Lemma B.2. With correlations, the argument essentially goes through unscathed given the estimates already proven in the lemmas. The recursion relation can then be plugged into the main text to derive critical properties.

Finally, for readers who are already familiar with the MHI argument in Ref. [48], we will make some occasional comments emphasizing essential ingredients here that are different from those in MHI. Our argument should be comprehensible without reading these comments.

1. Compact formula for $F_{\Lambda,\text{prod}}$

We start by writing down the production term without splitting it into disconnected and connected parts,

$$\begin{aligned}F_{\Lambda,\text{prod}}(l) = \int_{x\Lambda}^{\Lambda} d\Lambda' \frac{x_{\Lambda'}}{\langle d \rangle_{\Lambda'}} \int_{\Lambda'}^{l-\Lambda'(1+x^{-1})} \\ \times C^{TIT}_{\Lambda'}\left(l_1, \Lambda', l - \frac{\Lambda'}{x} - l_1\right) dl_1.\end{aligned} \tag{B20}$$

Following Ref. [48], we make a change of variables from $\Lambda' \to l_2 = l - \frac{\Lambda'}{x} - l_1$. Since x varies slowly with Λ, we can disregard the dependence of x on Λ and pull it out of the integrals. This allows us to simplify the production term

$$F_{\Lambda,\text{prod}}(l) \approx x^2 \int_D dl_2 dl_1 \frac{1}{\langle d \rangle_{\Lambda'}} C^{TIT}_{\Lambda'}(l_1, \Lambda', l_2), \tag{B21}$$

where the integration domain D is the blue isosceles triangle shown in Fig. 6. The integrand now involves a three-block correlation. We use the flow equation (A5) derived before to bound its growth in the region $x \max(l_1, l_2) \leqslant \Lambda' \leqslant \min(l_1, l_2)$ (this range is chosen so that we can drop the production term in (A5) involving integrals over five-block distributions),

$$\begin{aligned}\partial_{\Lambda'}\left(\frac{C^{TIT}_{\Lambda'}(l_1, \Lambda', l_2)}{\langle d \rangle_{\Lambda'}}\right) \approx -\frac{1}{\langle d \rangle^2_{\Lambda'}}\left[\rho^T_{\Lambda'}(\Lambda') + \mu^I_{\Lambda'}(\Lambda')\right]\langle d \rangle_{\Lambda'} C^{TIT}_{\Lambda'}(l_1, \Lambda', l_2) \\ + \frac{1}{\langle d \rangle_{\Lambda'}}\left\{C^{TIT}_{\Lambda'}(l_1, \Lambda', l_2)\left[\rho^T_{\Lambda'}(\Lambda') + \mu^I_{\Lambda'}(\Lambda')\right] - C^{TITI}_{\Lambda'}(l_1, \Lambda', l_2, \Lambda') \right. \\ \left. - C^{ITIT}_{\Lambda'}(\Lambda', l_1, \Lambda', l_2) + \partial_d C^{TIT}_{\Lambda'}(l_1, d, l_2)|_{d=\Lambda'}\right\}.\end{aligned} \tag{B22}$$

The first line cancels nicely with the first term on the second line. The remaining terms are

$$\partial_{\Lambda'}\left(\frac{C^{TIT}_{\Lambda'}(l_1, \Lambda', l_2)}{\langle d \rangle_{\Lambda'}}\right) \approx \frac{1}{\langle d \rangle_{\Lambda'}}\left\{-C^{TITI}_{\Lambda'}(l_1, \Lambda', l_2, \Lambda') - C^{ITIT}_{\Lambda'}(\Lambda', l_1, \Lambda', l_2) + \partial_d C^{TIT}_{\Lambda'}(l_1, d, l_2)|_{d=\Lambda'}\right\}. \tag{B23}$$

Using assumptions 2 and 3, all three terms can be bounded by $\frac{1}{\langle d \rangle_{\Lambda'}} C^{TIT}_{\Lambda'}(l_1, \Lambda', l_2)\rho^T_{\Lambda'}(\Lambda')x^c$. By an easy adaptation of the argument in Lemma B.2, we have the uniform estimate

$$\boxed{\frac{C^{TIT}_{\Lambda'}(l_1, \Lambda', l_2)}{\langle d \rangle_{\Lambda'}} \approx \text{const} \quad \forall \max(l_1, l_2)x \leqslant \Lambda' \leqslant \min(l_1, l_2).} \tag{B24}$$

Now we are ready to tackle the double integral over D (the blue + orange region in Fig. 6). The subset of the domain where $l_1, l_2 \geqslant \Lambda$ is an isosceles right triangle with leg length $\frac{\Lambda}{x} - x\Lambda$. Denote this right triangle by T and the remaining narrow wedges $D \setminus T$. Since the two narrow wedges are symmetric about the line $l_1 = l_2$, we need only demonstrate that

the integral over one of the wedges is suppressed relative to the integral over the right triangular domain. This can be accomplished in two steps:

(1) Let us consider first the right triangular domain T. The difficulty in estimating this integral is that the cutoff Λ' of the integrand depends implicitly on l_1, l_2. We would like to make a series of approximations until we can evaluate the integral at a fixed cutoff.

To do that, we first consider the orange square $[\Lambda, \frac{\Lambda}{2x}]\times[\Lambda, \frac{\Lambda}{2x}]$ contained in T. Outside of this square, $l_1 \geqslant \frac{\Lambda}{2x}$ or $l_2 \geqslant \frac{\Lambda}{2x}$, implying that $\Lambda' = \Lambda + x(2\Lambda - l_1 - l_2) \leqslant \frac{\Lambda}{2}$. As a result, $\frac{\Lambda'}{l_1} \leqslant x$ or $\frac{\Lambda'}{l_2} \leqslant x$. But since the least unlikely way to produce a large T block with $l_1 \geqslant \frac{\Lambda'}{x}$ is to combine two positively correlated T blocks at cutoff, $C^{TIT}_{\Lambda'}(l_1, \Lambda', l_2)$ must be exponentially decaying in l_1, l_2 for all $(l_1, l_2) \notin [\Lambda, \frac{\Lambda}{2x}]\times[\Lambda, \frac{\Lambda}{2x}]$ with a decay length on the order of $\frac{\Lambda'}{x}$. These exponential tails will give small corrections and for a leading-order approximation we can restrict the integral to the orange square from now on.

For readers familiar with MHI, note that our argument is *subtly different* from the original MHI argument that replaced the cutoff Λ' with Λ everywhere in the orange square. This replacement is puzzling because $x\max(l_1, l_2) \leqslant \Lambda' \leqslant \min(l_1, l_2)$ is "not true everywhere in D" and the analog of Lemma B.2 for uncorrelated RG cannot be applied. We circumvent this possible loophole by restricting to an even smaller square $S' = [\Lambda, \frac{\Lambda}{x^{1/2}}]\times[\Lambda, \frac{\Lambda}{x^{1/2}}]$. In this smaller domain, $x\max(l_1, l_2) = x^{1/2}\Lambda$, $\min(l_1, l_2) = \Lambda$ and $\Lambda' = \Lambda + 2x(\Lambda - l_1 - l_2) \leqslant \Lambda + 2x\Lambda - 2x^{1/2}\Lambda$. When $x \ll 1$, $x\max(l_1, l_2) \leqslant \Lambda' \leqslant \min(l_1, l_2)$ indeed holds and

$$\frac{C^{TIT}_{\Lambda'}(l_1, \Lambda', l_2)}{\langle d\rangle_{\Lambda'}} \approx \frac{C^{TIT}_{\Lambda}(l_1, \Lambda, l_2)}{\langle d\rangle_{\Lambda}} \quad \forall (l_1, l_2) \in S'. \tag{B25}$$

Within S', we can also estimate the decay of the integrand with l_1, l_2. Without loss of generality, let $l_1 \leqslant l_2$. By monotonicity of the probability distributions,

$$\frac{C^{TIT}_{\Lambda'}(l_1, \Lambda', l_2)}{\langle d\rangle_{\Lambda'}} \approx \frac{C^{TIT}_{\Lambda}(l_1, \Lambda, l_2)}{\langle d\rangle_{\Lambda}} \quad \forall l_1, l_2 \in \left[\Lambda, \frac{\Lambda}{x^{1/2}}\right]. \tag{B26}$$

For positive correlations, at cutoff l_1, $\langle d\rangle, \langle l\rangle \gg l_1, l_2$ and $C^{TIT}_{\Lambda}(l_1, \Lambda, l_2)$ should be enhanced relative to $\rho^T_\Lambda(l_1)\rho^T_\Lambda(l_2)\mu^I_\Lambda(\Lambda)$. However, the enhancement does not change the power law scaling in l_1, l_2 according to assumption 3. Therefore, by Lemma B.3, we have that along the separatrix,

$$\frac{C^{TIT}_{\Lambda'}(l_1, \Lambda', l_2)}{\langle d\rangle_{\Lambda'}} \sim O\left(\frac{1}{l_1^2 l_2^2}\right). \tag{B27}$$

When $(l_1, l_2) \in S \setminus S'$, we necessarily have $\frac{C^{TIT}_{\Lambda'}(l_1,\Lambda',l_2)}{\langle d\rangle_{\Lambda'}} \leqslant \frac{C^{TIT}_{\Lambda}(l_1,\Lambda,l_2)}{\langle d\rangle_{\Lambda}}$ since $\Lambda' < \Lambda$. The $\frac{1}{l_1^2 l_2^2}$ decay therefore guarantees that the contributions from the region $S \setminus S'$ is suppressed by a factor of x relative to the contributions from S' and can be thus neglected. Below the separatrix, the decay of $C^{TIT}_{\Lambda}(l_1, \Lambda, l_2)$ with l_1, l_2 has to be faster because flowing towards the MBL fixed line implies a clustering of T blocks close to the cutoff. Therefore, the suppression factor is much smaller than x and there is no additional complication.

After restricting to S, we can shift the cutoff uniformly to Λ so that

$$x^2\int_{S'} \frac{C^{TIT}_{\Lambda'}(l_1, \Lambda', l_2)}{\langle d\rangle_{\Lambda'}} \approx x^2\int_{S} \frac{C^{TIT}_{\Lambda}(l_1, \Lambda, l_2)}{\langle d\rangle_{\Lambda}}. \tag{B28}$$

Now up to errors that are suppressed by positive powers of x, we can extend the integration domain to $[\Lambda, \infty]^2$. Therefore, to leading order,

$$\begin{aligned} x^2\int_{S} \frac{C^{TIT}_{\Lambda}(l_1, \Lambda, l_2)}{\langle d\rangle_{\Lambda}} &= x^2\int_{[\Lambda,\infty]^2} \frac{1}{\langle d\rangle_{\Lambda}} C^{TIT}_{\Lambda}(l_1, \Lambda, l_2) \\ &= \frac{x^2\mu^I_\Lambda(\Lambda)}{\langle d\rangle_{\Lambda}}, \end{aligned} \tag{B29}$$

where the last identity follows from the definition of C^{TIT}_{Λ}.

(2) The integral over the narrow wedges is much easier to analyze. As explained above, the value of $C^{TIT}_{\Lambda'}(l_1, \Lambda', l_2)$ is only appreciable near $(l_1, l_2) = (\Lambda, \Lambda)$ and exponentially suppressed for $l_1, l_2 \geqslant \frac{\Lambda}{2x}$. But the area of the wedges restricted to $l_1, l_2 \leqslant \frac{\Lambda}{2x}$ is only $\mathcal{O}(x)$. Hence relative to the integral in the square region, the wedge integral must be suppressed at least by an additional factor of x. We thus arrive at equation (30) in the main text,

$$F_{\Lambda,\text{prod}} \approx \frac{x^2\mu^I_\Lambda(\Lambda)}{\langle d\rangle_{\Lambda}}. \tag{B30}$$

2. Bounding $F_{\Lambda,\text{depl}}$ relative to $F_{\Lambda,\text{prod}}$

At this point, it is easy to see that $F_{\Lambda,\text{depl}}$ is suppressed relative to $F_{\Lambda,\text{prod}}$. Recall that since the least unlikely way to create a T block late in the RG is by combining two T blocks of length $l^T \approx \Lambda$ with an insulating block with $l^I = \frac{\Lambda}{x}$, we expect $\rho^T_{x\Lambda}(l)$ to decay exponentially for $l > \mathcal{O}(\Lambda)$ (in fact we do not need it to be an exponential. A fast power law is enough). This means that

$$\frac{r_\Lambda(l)}{r_{x\Lambda}(l)} \approx \frac{\langle d\rangle_\Lambda \rho^T_\Lambda(l)}{\langle d\rangle_{x\Lambda}\rho^T_{x\Lambda}(l)} \approx \mathcal{O}(x^{-1}e^{1/x}) \gg 1, \tag{B31}$$

since $x \ll 1$, this immediately shows that $F_{\Lambda,\text{prod}}$ should dominate over $F_{\Lambda,\text{depl}}$. Hence we obtain the recursion relation

$$\boxed{r_\Lambda(l) = r_\Lambda(\Lambda/x) \approx \frac{x^2\mu^I_\Lambda(\Lambda)}{\langle d\rangle}.} \tag{B32}$$

Now using Lemma B.2, we can turn the above equation into a recursion relation for y,

$$\begin{aligned} y_{\Lambda/x} &= \frac{\Lambda^2}{x^2} r_{\Lambda/x}(\Lambda/x) \approx \frac{\Lambda^2}{x^2} r_\Lambda(\Lambda/x) \approx \frac{\Lambda^2}{x^2}\frac{x^2\mu^I_\Lambda}{\langle d\rangle} \\ &\approx \frac{\Lambda^2}{\langle d\rangle^2}\langle d\rangle\mu^I_\Lambda(\Lambda) = \left(\frac{y_\Lambda}{x}\right)^2\langle d\rangle\mu^I_\Lambda(\Lambda). \end{aligned} \tag{B33}$$

This recursion is the same as the uncorrelated recursion up to a factor $\langle d\rangle\mu^I_\Lambda(\Lambda)$.

APPENDIX C: EFFECTS OF LONG-RANGE CORRELATED DISORDER ON THE SYMMETRIC RG

In this Appendix, we expand upon a comment in Sec. VI about the effect of spatial correlations on earlier iterations

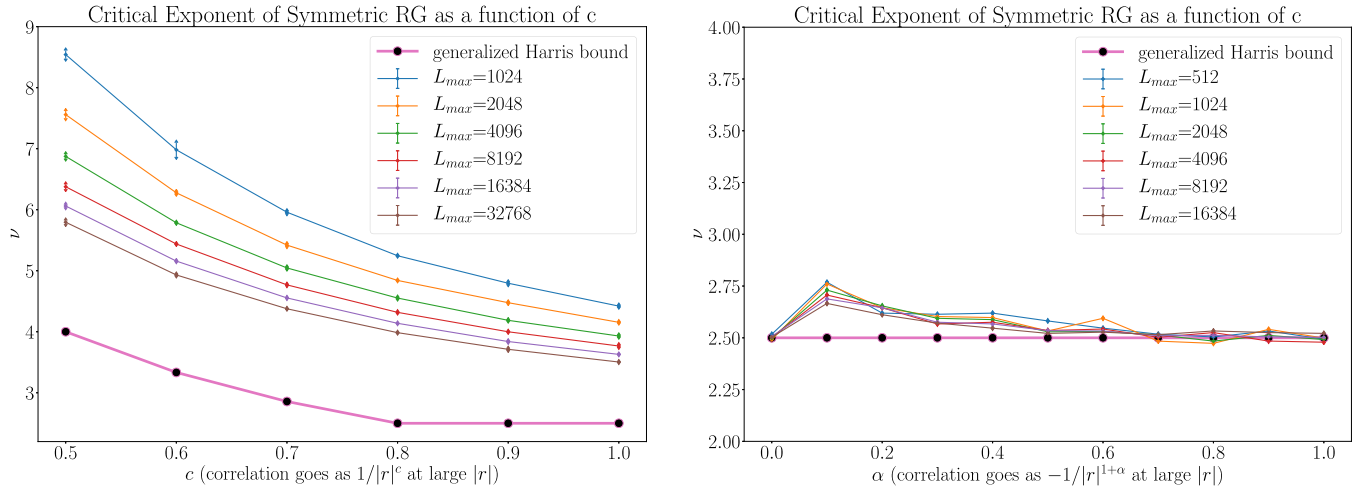

FIG. 7. The left/right panels show numerical estimates of ν for positive and hyperuniform correlations as a function of correlation strength as measured by c and maximum system size $L_{\max}$ used in the scaling collapse. For positive correlations, the critical exponent ν drifts down as $L_{\max}$ increases. In the accessible range of $L_{\max}$, we are not able to confirm whether the generalized Harris bound is saturated. For hyperuniform correlations, the finite-size effects are weaker since coherent fluctuations of large regions are suppressed. For $0.7 \lesssim \alpha$, we confirm that hyperuniform correlations do not change the uncorrelated value of ν, consistent with the general arguments in Sec. IV. For $\alpha < 0.7$, the numerical ν slightly exceeds the uncorrelated $\nu = 2.5$. This deviation is at the 10% level and much smaller than the deviation for positive correlations at any value of c. Thus we tentatively attribute it to finite-size effects.

of MBL RGs [25,28]. The RG rules in these models can be summarized as

$$l^I_{\text{new}} = l^I_{i-1} + \alpha_T l^T_i (= \Lambda) + l^I_{i+1}, \tag{C1}$$

$$l^T_{\text{new}} = l^T_{i-1} + \alpha_I l^I_i (= \Lambda) + l^T_{i+1}, \tag{C2}$$

where α_I, α_T are tunable parameters satisfying $\alpha = \alpha_I = \alpha_T^{-1}$. In the case of $\alpha = 1$ we recover the symmetric RG of Ref. [25].

Now we choose the initial block-length distributions so that $\langle l^T \rangle = W$ and $\langle l^I \rangle = 1$. For a particular α and spatial correlation, there is a critical $W_c(\alpha)$ where the production of T/I blocks exchange dominance. The critical exponent $\nu(\alpha)$ of the phase transition at $W = W_c(\alpha)$ can be extracted from a finite-size scaling analysis. From here on we focus on the symmetric RG with $\alpha_I = \alpha_T = W_c = 1$.

When correlations are turned on, we expect a shift to the critical exponent of the uncorrelated fixed point $\nu = 2.5$. When we turn on positive correlations, numerics show a clear upward drift in ν as $c \to 0$ (remember that c is the decay exponent of the initial correlations and small c corresponds to strong correlations). The numerical values for ν satisfy the generalized Harris bound, although a precise extrapolation of $\nu(L_{\max} \to \infty)$ is not possible due to finite-size effects (for concreteness, note the drifts shown in Fig. 7). For hyperuniform correlations, the numerically extracted values of ν stay close to $\nu = 2.5$ for all α, consistent with the general argument in Sec. IV that hyperuniform correlations should be irrelevant for asymptotically additive RG flows. At the special point at $\alpha = 1$, the wandering exponent $w = 0$ coincides with the wandering exponent of quasiperiodic correlations. Interestingly, the symmetric RG with quasiperiodic correlations have been shown to have $\nu = 1$ rather than $\nu = 2.5$ (see Ref. [57]). This means that as far as the symmetric RG is concerned, random disorder with $w = 0$ is qualitatively different from quasiperiodic disorder. Whether or not this qualitative difference exists for the MHI RG is an interesting question to address in the future.

[1] J. M. Deutsch, Phys. Rev. A **43**, 2046 (1991).
[2] M. Srednicki, Phys. Rev. E **50**, 888 (1994).
[3] L. D'Alessio, Y. Kafri, A. Polkovnikov, and M. Rigol, Adv. Phys. **65**, 239 (2016).
[4] R. Nandkishore and D. A. Huse, Annu. Rev. Condens. Matter Phys. **6**, 15 (2015).
[5] D. A. Abanin, E. Altman, I. Bloch, and M. Serbyn, Rev. Mod. Phys. **91**, 021001 (2019).
[6] S. Iyer, V. Oganesyan, G. Refael, and D. A. Huse, Phys. Rev. B **87**, 134202 (2013).
[7] V. Khemani, D. N. Sheng, and D. A. Huse, Phys. Rev. Lett. **119**, 075702 (2017).
[8] J. Z. Imbrie, Phys. Rev. Lett. **117**, 027201 (2016).
[9] V. Oganesyan and D. A. Huse, Phys. Rev. B **75**, 155111 (2007).
[10] A. Pal and D. A. Huse, Phys. Rev. B **82**, 174411 (2010).
[11] D. A. Huse, R. Nandkishore, and V. Oganesyan, Phys. Rev. B **90**, 174202 (2014).
[12] M. Serbyn, Z. Papi, and D. A. Abanin, Phys. Rev. Lett. **111**, 127201 (2013).
[13] S. J. Garratt and J. T. Chalker, Phys. Rev. Lett. **127**, 026802 (2021)
[14] A. Altland and T. Micklitz, Phys. Rev. Lett. **118**, 127202 (2017).
[15] D. J. Luitz, N. Laflorencie, and F. Alet, Phys. Rev. B **91**, 081103(R) (2015).

[16] X. Yu, D. J. Luitz, and B. K. Clark, Phys. Rev. B **94**, 184202 (2016).
[17] V. Khemani, S.-P. Lim, D. N. Sheng, and D. A. Huse, Phys. Rev. X **7**, 021013 (2017).
[18] R. K. Panda, A. Scardicchio, M. Schulz, S. R. Taylor, and M. Žnidarič, Europhys. Lett. **128**, 67003 (2020).
[19] P. Sierant, M. Lewenstein, and J. Zakrzewski, Phys. Rev. Lett. **125**, 156601 (2020).
[20] A. B. Harris, J. Phys. C **7**, 1671 (1974).
[21] J. T. Chayes, L. Chayes, D. S. Fisher, and T. Spencer, Phys. Rev. Lett. **57**, 2999 (1986).
[22] A. Chandran, C. R. Laumann, and V. Oganesyan, Finite size scaling bounds on many-body localized phase transitions, (2015).
[23] R. Vosk, D. A. Huse, and E. Altman, Phys. Rev. X **5**, 031032 (2015).
[24] A. C. Potter, R. Vasseur, and S. A. Parameswaran, Phys. Rev. X **5**, 031033 (2015).
[25] L. Zhang, B. Zhao, T. Devakul, and D. A. Huse, Phys. Rev. B **93**, 224201 (2016).
[26] P. T. Dumitrescu, R. Vasseur, and A. C. Potter, Phys. Rev. Lett. **119**, 110604 (2017).
[27] T. Thiery, M. Mller, and W. D. Roeck, arXiv:1711.09880.
[28] A. Goremykina, R. Vasseur, and M. Serbyn, Phys. Rev. Lett. **122**, 040601 (2019).
[29] A. Morningstar and D. A. Huse, Phys. Rev. B **99**, 224205 (2019).
[30] S.-K. Ma, C. Dasgupta, and C.-K. Hu, Phys. Rev. Lett. **43**, 1434 (1979).
[31] D. S. Fisher, Phys. Rev. Lett. **69**, 534 (1992).
[32] D. S. Fisher, Phys. Rev. B **51**, 6411 (1995).
[33] F. Igloi and C. Monthus, Phys. Rep. **412**, 277 (2005).
[34] F. Iglói and C. Monthus, Eur. Phys. J. B **91**, 290 (2018).
[35] A. Samanta, A. Chakraborty, and R. Sensarma, Phys. Rev. B **106**, L060201 (2022).
[36] P. J. D. Crowley and A. Chandran, SciPost Phys. **12**, 201 (2022).
[37] A. Morningstar, L. Colmenarez, V. Khemani, D. J. Luitz, and D. A. Huse, Phys. Rev. B **105**, 174205 (2022).
[38] S. J. Garratt, S. Roy, and J. T. Chalker, Phys. Rev. B **104**, 184203 (2021).
[39] D. M. Basko, I. L. Aleiner, and B. L. Altshuler, Ann. Phys. **321**, 1126 (2006).
[40] J. Šuntajs, J. Bonča, T. Prosen, and L. Vidmar, Phys. Rev. E **102**, 062144 (2020).
[41] D. Sels and A. Polkovnikov, Phys. Rev. E **104**, 054105 (2021).
[42] D. Abanin, J. Bardarson, G. De Tomasi, S. Gopalakrishnan, V. Khemani, S. Parameswaran, F. Pollmann, A. Potter, M. Serbyn, and R. Vasseur, Ann. Phys. **427**, 168415 (2021).
[43] W. De Roeck and F. Huveneers, Phys. Rev. B **95**, 155129 (2017).
[44] L. Herviou, S. Bera, and J. H. Bardarson, Phys. Rev. B **99**, 134205 (2019).
[45] N. Laflorencie, G. Lemarié, and N. Macé, Phys. Rev. Res. **2**, 042033(R) (2020).
[46] J. Šuntajs, J. Bonča, T. Prosen, and L. Vidmar, Phys. Rev. B **102**, 064207 (2020).
[47] S. Roy and D. E. Logan, Phys. Rev. B **104**, 174201 (2021).
[48] A. Morningstar, D. A. Huse, and J. Z. Imbrie, Phys. Rev. B **102**, 125134 (2020).
[49] F. Setiawan, D.-L. Deng, and J. H. Pixley, Phys. Rev. B **96**, 104205 (2017).
[50] M. Lee, T. R. Look, S. P. Lim, and D. N. Sheng, Phys. Rev. B **96**, 075146 (2017).
[51] E. V. H. Doggen and A. D. Mirlin, Phys. Rev. B **100**, 104203 (2019).
[52] M. Žnidarič and M. Ljubotina, Proc. Natl. Acad. Sci. USA **115**, 4595 (2018).
[53] V. K. Varma and M. Žnidarič, Phys. Rev. B **100**, 085105 (2019).
[54] H. Singh, B. Ware, R. Vasseur, and S. Gopalakrishnan, Phys. Rev. B **103**, L220201 (2021).
[55] T. Chanda, P. Sierant, and J. Zakrzewski, Phys. Rev. B **101**, 035148 (2020).
[56] A. S. Aramthottil, T. Chanda, P. Sierant, and J. Zakrzewski, Phys. Rev. B **104**, 214201 (2021).
[57] U. Agrawal, S. Gopalakrishnan, and R. Vasseur, Nat. Commun. **11**, 2225 (2020).
[58] S.-X. Zhang and H. Yao, Phys. Rev. Lett. **121**, 206601 (2018).
[59] M. Titov and H. Schomerus, Phys. Rev. Lett. **95**, 126602 (2005).
[60] A. Croy, P. Cain, and M. Schreiber, Eur. Phys. J. B **82**, 107 (2011).
[61] P. Lugan, A. Aspect, L. Sanchez-Palencia, D. Delande, B. Grémaud, C. A. Müller, and C. Miniatura, Phys. Rev. A **80**, 023605 (2009).
[62] F. M. Izrailev, A. A. Krokhin, and N. Makarov, Phys. Rep. **512**, 125 (2012).
[63] E. Fratini and S. Pilati, Phys. Rev. A **92**, 063621 (2015).
[64] U. Agrawal, S. Gopalakrishnan, and R. Vasseur, Phys. Rev. Lett. **125**, 265702 (2020).
[65] A. Chandran, C. R. Laumann, and V. Oganesyan, arXiv:1509.04285.
[66] J. M. Luck, Europhys. Lett. **24**, 359 (1993).
[67] A. Weinrib, Phys. Rev. B **29**, 387 (1984).
[68] A. Weinrib and B. I. Halperin, Phys. Rev. B **27**, 413 (1983).
[69] P. T. Dumitrescu, A. Goremykina, S. A. Parameswaran, M. Serbyn, and R. Vasseur, Phys. Rev. B **99**, 094205 (2019).
[70] P. J. D. Crowley, C. R. Laumann, and S. Gopalakrishnan, Phys. Rev. B **100**, 134206 (2019).
[71] J. Yvon, *La théorie statistique des fluides et l'équation d'état*, Vol. 203 (Hermann & Cie, Paris, 1935).
[72] N. N. Bogoliubov, J. Phys. USSR **10**, 265 (1946).
[73] J. G. Kirkwood, J. Chem. Phys. **14**, 180 (1946).
[74] J. G. Kirkwood, J. Chem. Phys. **15**, 72 (1947).
[75] M. Born and H. S. Green, *A General Kinetic Theory of Liquids* (CUP Archive, Cambridge, 1949).